Organic Geochemistry 83-84 (2015) 27–53

Contents lists available at ScienceDirect

Organic Geochemistry

journal homepage: www.elsevier.com/locate/orggeochem

Evaluation of the petroleum composition and quality with increasing thermal maturity as simulated by hydrous pyrolysis: A case study using a Brazilian source rock with Type I kerogen

André L.D. Spigolon [a,d,*], Michael D. Lewan [b], Henrique L. de Barros Penteado [c], Luiz Felipe C. Coutinho [d], João G. Mendonça Filho [e]

[a] Universidade Federal do Rio de Janeiro, Instituto de Geociências, Av. Athos da Silveira, 274, Prédio do CCMN, Cidade Universitária, 21.949-900 Rio de Janeiro, RJ, Brazil
[b] U.S. Geological Survey (Emeritus), Box 25046, MS 977, Denver Federal Center, Denver, CO 80225, USA
[c] Basin and Petroleum System Modeling (Petrobras/E&P-EXP), Av. República do Chile, 330, Centro, 20.031-117 Rio de Janeiro, RJ, Brazil
[d] Division of Geochemistry, Petrobras Research and Development Center (CENPES), Av. Horácio Macedo, 950, Cidade Universitária, 21.941-915 Rio de Janeiro, RJ, Brazil
[e] Palynofacies and Organic Facies Laboratory (LAFO)/DEGL/IGEO/CCMN/UFRJ, Av. Athos da Silveira, 274 – Prédio do CCMN, Sala JI-020, Cidade Universitária, 21.941-916 Rio de Janeiro, RJ, Brazil

ARTICLE INFO

Article history:
Received 26 October 2014
Received in revised form 13 February 2015
Accepted 2 March 2015
Available online 10 March 2015

Keywords:
Brazilian Type I kerogen
Hydrous pyrolysis
Thermal maturation
Generation and expulsion
Petroleum composition and quality
API gravity
Sulfur content
Asphaltenes
Saturates
Gas/oil ratio

ABSTRACT

Hydrous pyrolysis (HP) experiments were used to investigate the petroleum composition and quality of petroleum generated from a Brazilian lacustrine source rock containing Type I kerogen with increasing thermal maturity. The tested sample was of Aptian age from the Araripe Basin (NE-Brazil). The temperatures (280–360 °C) and times (12–132 h) employed in the experiments simulated petroleum generation and expulsion (i.e., oil window) prior to secondary gas generation from the cracking of oil. Results show that similar to other oil prone source rocks, kerogen initially decomposes in part to a polar rich bitumen, which decomposes in part to hydrocarbon rich oil. These two overall reactions overlap with one another and have been recognized in oil shale retorting and natural petroleum generation. During bitumen decomposition to oil, some of the bitumen is converted to pyrobitumen, which results in an increase in the apparent kerogen (i.e., insoluble carbon) content with increasing maturation.

The petroleum composition and its quality (i.e., API gravity, gas/oil ratio, C_{15+} fractions, alkane distribution, and sulfur content) are affected by thermal maturation within the oil window. API gravity, C_{15+} fractions and gas/oil ratios generated by HP are similar to those of natural petroleum considered to be sourced from similar Brazilian lacustrine source rocks with Type I kerogen of Lower Cretaceous age. API gravity of the HP expelled oils shows a complex relationship with increasing thermal maturation that is most influenced by the expulsion of asphaltenes. C_{15+} fractions (i.e., saturates, aromatics, resins and asphaltenes) show that expelled oils and bitumen are compositionally separate organic phases with no overlap in composition. Gas/oil ratios (GOR) initially decrease from 508–131 m^3/m^3 during bitumen generation and remain essentially constant (81–84 m^3/m^3) to the end of oil generation. This constancy in GOR is different from the continuous increase through the oil window observed in anhydrous pyrolysis experiments. Alkane distributions of the HP expelled oils are similar to those of natural crude oils considered to be sourced from similar Brazilian lacustrine source rocks with Type I kerogen of Lower Cretaceous age. Isoprenoid and *n*-alkane ratios (i.e., pristane/*n*-C_{17} and phytane/*n*-C_{18}) decrease with increasing thermal maturity as observed in natural crude oils. Pristane/phytane ratios remain constant with increasing thermal maturity through the oil window, with ratios being slightly higher in the expelled oils relative to those in the bitumen. Generated hydrocarbon gases are similar to natural gases associated with crude oils considered to be sourced from similar Brazilian lacustrine source rocks with Type I kerogen of Lower Cretaceous, with the exception of elevated ethane contents. The general overall agreement in composition of natural and hydrous pyrolysis petroleum of lacustrine source rocks observed in this study supports the utility of HP to better characterize petroleum systems and the effects of maturation and expulsion on petroleum composition and quality.

* Corresponding author at: Division of Geochemistry, Petrobras Research and Development Center (CENPES), Av. Horácio Macedo, 950, Cidade Universitária, 21.941-915 Rio de Janeiro, RJ, Brazil. Tel.: +55 21 2162 4384; fax: +55 21 2162 6799.
E-mail address: andrespigolon@petrobras.com.br (A.L.D. Spigolon).

http://dx.doi.org/10.1016/j.orggeochem.2015.03.001
0146-6380/

1. Introduction

Many geological factors contribute to petroleum composition, and thus its economic value, which is related to the original kerogen composition, thermal evolution of its source rock and secondary processes affecting petroleum during migration and accumulation. Furthermore, the prediction of the quality and quantity of oil and gas generated from a given kerogen prior to drilling remains a key issue in petroleum exploration (e.g. Behar et al., 1997). To minimize these uncertainties and to understand petroleum formation process and petroleum compositional variations with increasing maturation, the petroleum industry has used laboratory pyrolysis experiments to artificially mature source rocks at relatively high temperatures and short times under an inert atmosphere (e.g. Rock–Eval pyrolysis, pyrolysis–gas chromatography, gold tube pyrolysis, micro-scale sealed vessel pyrolysis and hydrous pyrolysis). These artificial maturation techniques allow us to study the effect of several conditions present in the natural system that influence the generation, expulsion and composition of petroleum (e.g. temperature, time, pressure, presence of water, source rock mineralogy, retention), as well as to determine kinetic models that when extrapolated to geological conditions (lower temperatures and longer times), determine the timing and extent of petroleum generation in a sedimentary basin.

Because different pyrolysis techniques and experimental conditions are used in these studies (e.g. open or closed system, hydrous or anhydrous conditions, pressure, isothermal or nonisothermal heating), significant differences have been observed. The differences are more notable between open and closed systems regarding the composition of generated petroleum products, although overall the amounts generated can be similar (Lewan, 1993a, 1994, 1997; Behar et al., 1997, 2010; Lewan and Ruble, 2002). Open system pyrolysis conditions appear to cause an overlap of reactions leading to the generation of bitumen and immiscible oil, with the collective and the petroleum product having a dominance of polar compounds, represented by the S_2 peak of the Rock–Eval pyrolysis (Behar et al., 1997). Conversely, geochemical studies have demonstrated that the artificial maturation in closed systems generates a natural looking petroleum (Lewan et al., 1979; Monthioux et al., 1985; Horsfield et al., 1989). This similarity can be attributed to the cracking of polar compounds (i.e., non-hydrocarbons of very high molecular weight: resins and asphaltenes) to hydrocarbons of lower molecular weight, such as saturated and aromatic compounds (Ruble et al., 2001; Behar et al., 2008, 2010).

These experimental techniques operate at the lowest possible temperatures for laboratory pyrolysis experiments (280–365 °C), but hydrous pyrolysis (HP) is the only technique that provides expelled oil (Lewan and Ruble, 2002). Unlike dry closed pyrolysis methods, HP generates a pyrolyzate that is compositionally similar to natural crude oils and differentiates between bitumen and oil that is expelled in a manner that is operative in the subsurface of sedimentary basins (Lewan, 1997; Lewan and Roy, 2011).

Expelled oils generated from HP are enriched in hydrocarbons mainly as a result of the thermal decomposition of bitumen (i.e., resins and asphaltenes), which is an intermediate thermal product derived from the decomposition of kerogen (e.g. Franks and Goodier, 1922; Allred, 1966; Tissot, 1969; Tissot and Espitalié, 1975; Lewan, 1985). The presence of water has been considered critical in experimental and natural oil generation as a source of hydrogen and in the development of expelled oil and gas (Lewan, 1997; Schimmelmann et al., 1999, 2001). As a consequence of thermal stress, covalent bonds within the bitumen break and a hydrocarbon enriched oil is generated. The immiscibility of the generated oil with the water-saturated bitumen and the accompanying net volume increase results in the expulsion of the generated oil from the rock (Lewan, 1994, 1997; Lewan and Ruble, 2002). According to these authors, this suggests that the expulsion mechanism simulated by HP is in agreement with the concept that oil expulsion is a consequence of its generation within a rock as originally proposed by Momper (1978). Without the presence of liquid water during pyrolysis, no hydrocarbon enriched oil is differentiated from polar enriched bitumen, and no net volume increase occurs to expel the oil from the bitumen impregnated rock. This is based on direct experimental comparisons as described in detail by Lewan (1997) and Lewan and Roy (2011). Moreover, this technique has also shown to provide useful information on the primary migration, stages and kinetics of petroleum generation, and thermal maturation indices (Lewan, 1983, 1985, 1987; Winters et al., 1983; Soldan et al., 1988). For these reasons, HP is the most appropriate pyrolysis method to simulate petroleum generation and expulsion, which are the reason it is used in this study to evaluate changes in petroleum composition and quality with increase of thermal maturity.

Only a few studies have addressed the issue of predicting the petroleum composition and its quality using anhydrous pyrolysis data as discussed by Duppenbecker and Horsfield (1990), di Primio et al. (1998), Santamaría-Orozco and Horsfield (2003), di Primio and Horsfield (2006), Penteado and Araujo (2012), Tan et al. (2013) and Abbassi et al. (2014). However, no work has integrated physical and chemical properties of expelled oils and gases predicted by artificial maturation by hydrous pyrolysis and compared them to natural petroleum from similar source rocks.

The aim of the present work is to apply hydrous pyrolysis using different time–temperature conditions (280–365 °C and 12–132 h) to investigate changes in oil and gas properties with increasing maturity in the primary stage of oil generation from a Lower Cretaceous Brazilian source rock containing Type I kerogen. Special emphasis was given to the quantification and characterization of the original organic matter contained in the aliquots subjected to hydrous pyrolysis, and to the various products of the experiments (residual rock, bitumen, expelled oil and gas). A thorough analytical workflow was designed to allow for the determination of bulk, compositional, and molecular geochemical properties of the residual organic matter and the petroleum generated and expelled after each experiment. The changes in geochemical properties of expelled oil and gas include gas/oil ratio (GOR), API gravity, sulfur content, gas composition (C_1–C_5), volatile fraction (C_6–C_{14} SAT + ARO), C_{15+} SARA fractions (saturates, aromatics, resins and asphaltenes) and molecular indices. These properties were evaluated and discussed as a function of the transformation ratio (TR) for oil generation, which provided insights into the composition and mechanisms of petroleum formation as well as the controls on oil and gas quality. The expelled oils and gases were also compared to natural petroleum compositions from similar source rocks to test the applicability of the laboratory data to support petroleum system characterization.

In addition to the above stated objectives, this study also broadens our geochemical perspective of petroleum formation from Brazilian lacustrine source rocks containing Type I kerogen. Characterization of Type I kerogen and its petroleum has relied heavily on lacustrine source rocks and their petroleum in the Eocene Green River Formation of the Uinta Basin (e.g., Espitalié et al., 1985; Ruble et al., 2001, and references therein). However, the actual amount of oil attributed to this kerogen type in the Uinta Basin (0.7 billion barrels of oil have been produced; Utah Geological Survey, 2014) pales in comparison to petroleum produced from lacustrine Brazilian source rocks containing Type I kerogen. The lacustrine source rocks with Type I kerogen in the Brazilian Campos and Santos basins alone are responsible for more than 5.5 billion barrels of produced oil between 2004 and 2013,

with proved oil reserves of 13 billion barrels (ANP, 2014). Comparisons are made in this study between the pyrolysis products from Brazilian Type I kerogen and Green River Type I kerogen where published data are available and appropriate for comparisons.

2. Sampling and methods

2.1. Sample collection, preparation and characterization

An outcrop sample of an organic rich immature source rock of the Batateira Beds of the Barbalha Formation was collected along the course of the Batateira River in the State of Ceará (Crato City), in the Araripe Basin, northeastern Brazil, which is an onshore basin composed mostly of Late Jurassic and Early Cretaceous sediments (Fig. 1).

The name "Batateira Beds" was initially proposed by Hashimoto et al. (1987) to designate an interval with black bituminous shales associated with carbonate concretions of Neoaptian age (P-270 biozone; Lima and Perinotto, 1984). Due to the huge lateral extension and limited thickness (< 10 m), the deposition of the Batateira Beds constitutes a stratigraphic marker of regional importance in the Araripe Basin that represents the first record of a lacustrine system with anoxic conditions responsible for the significant preservation of organic matter (Assine, 2007). A detailed description of the Barbalha Formation was previously reported by Chagas et al. (2007).

The difficulty in obtaining core samples of immature source rocks in large quantities for HP experiments (~10 kg), especially for the deeply buried syn-rift lacustrine source rocks along the marginal basins necessitates the choice of this organic rich sample as a reasonable analog for Brazilian lacustrine source rocks from the Lower Cretaceous.

According to Katz and Mello (2000), approximately 95% of discovered Brazilian oils were generated from lacustrine source rocks related to the rift phase. This number may be higher considering the recent discoveries of pre-salt accumulations. Additionally, the organic richness indicated by values as high as 37% total organic carbon (TOC) would assure that adequate amounts of expelled oil would be generated by HP.

Sample collection and preparation is one of the most important steps to ensure the success of the HP experiments and the reproducibility of the results.

A large amount of sample (10 kg) was collected directly from the outcrop, taking care with the huge vertical variations to avoid compositional heterogeneities. The ideal situation is to restrict the collection to an interval only a few centimeters thick (10–20 cm) within rock layers or beds exposed to minimal weathering, according to the procedures recommended by Lewan (1980). The immature source rock sample was reduced in size to aliquots of approximately 200 g. One small aliquot (1–2 g) was taken from each set of samples for TOC and Rock–Eval (RE) analyses in order to verify the heterogeneity in the measured organic parameters, especially organic content (TOC in wt%) and petroleum generation potential (Rock–Eval S_2 peak in mg/g rock). Based on the statistical analysis, it was possible to discard the samples with TOC and S_2 values less or greater than one standard deviation from the average values.

For TOC and RE analyses, the aliquots of unheated sample were pulverized and sieved in an 80 mesh size. Inorganic carbon was removed with hydrochloric acid and TOC contents were determined

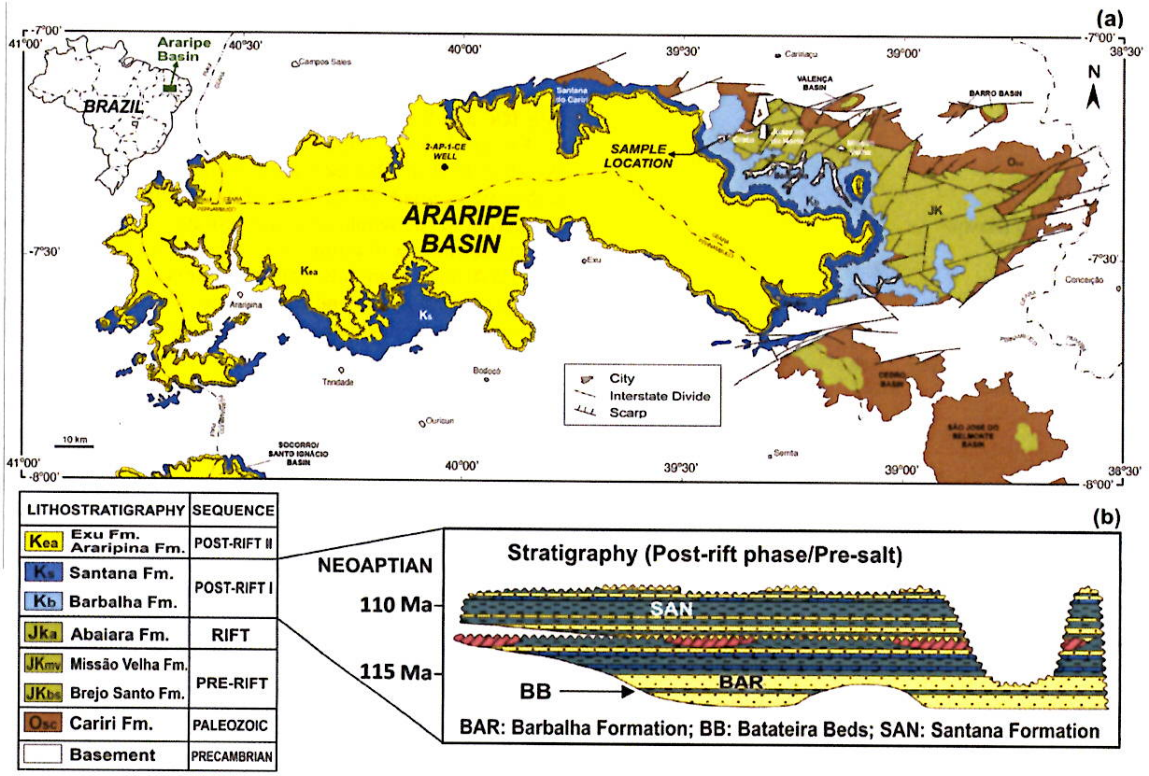

Fig. 1. (a) Geological map of Araripe Basin and location of the studied sample. (b) Stratigraphic section of Post-rift phase with the interval representing Batateira Beds (based on Assine, 2007).

by combustion in a Leco SC-144 carbon analyzer with an infrared detector. The insoluble residue (IR%) was calculated using insoluble sample weight (ISW) divided by original sample weight (OSW) multiplied by 100. Rock–Eval geochemical parameters were obtained with a Rock–Eval 6 instrument (Behar et al., 2001).

Sample preparation continued with the crushing and sieving of whole samples to gravel size ranging from 5–30 mm, followed by mixing, homogenization and quartering. Four aliquots of each quarter were taken for TOC and RE analyses to verify their heterogeneity. The average of the sixteen results must have a standard deviation below 10% for the sample to be considered homogeneous. If the samples show some heterogeneity, the procedure was repeated until the samples exhibit homogeneous geochemical characteristics within the 10% limit. Subsequently, a series of inorganic and organic geochemical analyses were employed to determine the original characteristics of the homogeneous sample. Table 1 summarizes the geochemical analyses characterizing the original rock and its kerogen.

X-ray diffraction was used to characterize total and clay mineralogy of the original rock using RIGAKU D/MAX – 2200/PC. The analytical setting was k-alpha radiation of copper under the conditions of 40 kV and 40 mA current filament and crevices 2 mm, 2 mm, 0.3 mm and 0.6 mm. The scanning speed of the goniometer was 6 degrees/min for clay and 2.33 degrees/min for total mineralogy. The qualitative analysis of each mineral was obtained using Jade 5 software (Materials Data Incorporated Company) and the mineral database of International Centre for Diffraction Data.

Vitrinite reflectance measurements were performed on a single block of extracted rock using a Carl Zeiss Axioskop 2 Plus microscope equipped with a J&M spectrophotometer (MSP 200). The single block was prepared and polished with rock fragments of approximately 2 mm in size embedded in resin. Reference reflectance standards from Klein & Beckers were used to calibrate the microscope. Measurements of mean random vitrinite reflectance ($\%R_o$) were performed in particles of vitrodetrinite with 50× objective using immersion oil Imersöl 518 F (n_e = 1.518; 23 °C) according to standards (ISO 7404-5; DIN 22020-5 and ASTM). The analyses were performed at a room temperature of 23 °C ± 1 °C.

Kerogen was isolated from original rock using HCl (37%) and HF (40%) cold acid attacks to remove the mineral fraction, mostly carbonates and silicates, followed by neutralization with filtered water in each step. A new acid attack with hot HCl (37%) is performed to remove any mineral residue. Then, the kerogen is dried using a lyophilizer and submitted to X-ray diffraction at the same conditions described above in order to verify inorganic mineral traces associated with organic matter that can contribute with some inorganic mass in the elementary analysis of kerogen. If some inorganic traces were found in the kerogen (mostly calcite, ralstonite and clay minerals), the sample needs to be treated again with hot HCl acid attack to remove this inorganic residues. At the end, the cleaned and dried kerogen was submitted to elementary analysis (C, H, N, S, O, and Fe) in Huffman Labs (Golden, CO). The organic matter concentrated was also used to mount strewn slides for palynofacies analysis (Tyson, 1995).

Stable carbon isotopes ($\delta^{13}C$, ‰) of original kerogen were determined using a Thermo Finnigan Flash 1112 Series Elemental Analyzer coupled to a Finnigan MAT 252 Isotope Ratio Mass Spectrometer (EA-IRMS).

The tested sample is very rich in organic matter, with a TOC of 28.5%, and contains a Type I kerogen, as shown by the atomic elemental ratios of kerogen (H/C, O/C and $S_{org}/[S_{org} + C]$) and RE parameters of whole rock (hydrogen index, HI and oxygen index, OI). The amount of organic sulfur in the kerogen (i.e., $S_{org}/[S_{org} + C] = 0.014$) is relatively high for a Type I kerogen compared to that reported for Green River source rocks (e.g., $S_{org}/[S_{org} + C] = 0.002$; Lewan and Ruble, 2002). The thermal immaturity is indicated by the high kerogen atomic H/C ratio and HI (1.5 mg S_2/g TOC and 893 mg S_2/g TOC, respectively), and very low values of RE production indices (PI = 0.02) and vitrinite reflectance (R_o = 0.40%). Mass balance after dilute HCl treatment suggests a carbonate content of 30–40%. Complementary analysis of X-ray diffraction in the whole rock corroborates the presence of carbonate in the mineral fraction and indicates a calcite content of 40% with 26% clay minerals (mostly interstratified illite/smectite), 24% quartz, 7% pyrite and 3% gypsum. This fine grained rock is a carbonaceous argillaceous marlstone, based on the classification proposed by Lewan (1978).

Twenty-five 150 g aliquots were randomly prepared from the homogenized sample. Each aliquot was dried in a fume hood for several hours before starting the hydrous pyrolysis experiments to minimize possible variation in moisture contents. In this set of samples, the moisture loss was determined gravimetrically with an average of 3.2%. For a maximum control of the original organic parameters of each of the 25 aliquots, a small sub-aliquot (1–2 g) was taken for final TOC and RE analyses. Table 2 contains the original organic parameters measured for each of these sub-aliquots, which were ultimately used to calculate the product yields after each hydrous pyrolysis experiment, on an original total organic carbon (TOC_o) basis.

Table 1
Geochemical characterization of the original sample.

Kerogen analyses	
% Carbon[a]	75.2
% Hydrogen[a]	9.5
% Oxygen[a]	10.8
% Nitrogen[a]	1.7
% Sulfur (organic)[a]	2.8
Atomic H/C ratio[a]	1.50
Atomic O/C ratio[a]	0.11
Atomic $S_{org}/[S_{org} + C]$ ratio[a]	0.014
$\delta^{13}C$ (per mil, PDB)	−29.9
Amorphous organic matter (AOM)%[b]	78
Phytoclasts% [b]	15
Palynomorphs%[b]	7
Kerogen classification	Type I
Whole rock analyses	
Total organic carbon (TOC wt%)	28.5
Vitrinite reflectance (mean random $\%R_o$)	0.40
Number of vitrinite reflectance measurements	28
S_1 (mg/g rock)[c]	5.7
S_2 (mg/g rock)[c]	255
S_3 (mg/g rock)[c]	2.6
S_1/TOC × 100 (mg/g TOC)[c]	20
HI (mg S_2/g TOC)[c]	895
OI (mg S_3/g TOC)[c]	9.2
PI ($S_1/[S_1 + S_2]$)[c]	0.02
T_{max} (°C)[c]	422
% Calcite[d]	40
% Quartz[d]	24
% Clay (interstratified illite/smectite)[d]	26
% Pyrite[d]	7
% Gypsum[d]	3
Rock classification	Carbonaceous argillaceous marlstone

[a] Elemental analyses.
[b] Palynofacies analysis.
[c] Rock–Eval pyrolysis.
[d] X-ray diffraction.

2.2. Hydrous pyrolysis experiments

Hydrous pyrolysis (HP) is a closed system method for thermally decomposing organic matter in the presence of liquid water (Lewan et al., 1979).

Table 2
Original organic parameters determined for each experiment (unheated samples).

HP number	Temperature (°C)	Time (h)	Weight of rock (g)	TOC_o (wt%)	TOC_o of sample (g)	S_1[a]	S_2[a]	S_3[a]	HI[a]	OI[a]
Temperature series										
3648	280	72	147.4	31.2	46.0	5.0	280.4	1.2	898.7	3.8
3630	300	72	150.9	32.6	49.2	5.2	268.6	2.0	823.9	6.1
3645	310	72	148.9	30.8	45.9	5.5	246.1	2.4	799.0	7.8
3632	320	72	147.9	29.5	43.6	5.8	255.3	2.3	865.4	7.8
3667	325	72	148.4	28.9	42.9	4.8	261.9	3.7	906.2	12.8
3649	330	72	148.3	27.5	40.8	6.3	258.9	2.3	941.5	8.4
3668	340	72	147.9	27.8	41.1	6.0	250.9	4.1	902.5	14.7
3650	345	72	149.1	25.6	38.2	5.4	226.2	4.1	883.6	16.0
3652	350	72	148.5	28.3	42.0	5.1	255.0	3.6	901.1	12.7
3646	355	72	147.8	28.1	41.5	6.0	240.1	2.4	854.4	8.5
3631	360	72	147.6	26.9	39.7	5.4	241.3	1.5	897.0	5.6
3647	365	72	151.7	27.0	41.0	5.5	240.2	2.0	889.6	7.4
Time series										
3666	310	36	147.6	28.3	41.8	5.9	265.8	3.1	939.2	11.0
3658		104	148.7	28.4	42.2	5.5	261.0	2.9	919.0	10.2
3671		132	148.6	28.4	42.2	6.5	268.6	2.3	945.8	8.1
3669	325	24	152.6	28.6	43.6	5.2	222.0	2.7	776.2	9.4
3662		48	152.8	28.6	43.7	5.6	263.5	1.0	921.3	3.5
3659		104	148.8	29.4	43.7	6.8	261.4	1.8	889.1	6.1
3673		120	152.5	29.2	44.5	6.2	257.5	3.0	881.8	10.3
3670	340	24	148.3	27.6	40.9	5.0	252.4	3.6	914.5	13.0
3663		48	150.8	27.4	41.3	5.4	250.7	3.0	915.0	10.9
3660		96	147.2	27.6	40.6	5.7	254.6	2.8	922.5	10.1
3665	355	12	153.1	28.5	43.6	5.7	258.6	2.8	907.4	9.8
3672		30	150.5	28.4	42.7	5.9	261.6	2.2	921.1	7.7
3664		48	148.7	28.3	42.1	6.0	264.5	2.6	934.6	9.2
			Mean	28.5	42.6	5.7	255.0	2.6	895.0	9.2
			SD	1.4	2.3	0.5	13.2	0.8	42.5	3.1

[a] Rock–Eval pyrolysis: S_1 = free volatile hydrocarbons (in mg/g rock), S_2 = original petroleum generation potential (in mg/g rock), S_3 = CO_2 from organic source (in mg/g rock), HI = hydrogen index (in mg S_2/g TOC), OI = oxygen index (in mg CO_2/g TOC); HP = hydrous pyrolysis; TOC_o = original total organic carbon; SD = standard deviation.

The experiments were conducted in one liter Hastelloy C-276 reactors (Parr Instruments Company), which were loaded with 147.2–152.8 g of homogeneous, organic rich rock and 400 g of distilled and, deionized water. The amount of water is calculated based on the bulk density of rock (1.5 g/cm^3) to ensure that the rock is submerged in liquid water at subcritical experimental temperatures (< 374 °C), and also to keep the volume of water expansion at the lowest (280 °C) and highest (365 °C) temperatures below the total volume of the reactor (~1025 cm^3) for safety (Lewan, 1993a).

After loading and sealing the reactor, the remaining headspace was evacuated to < 0.5 psia and filled with about 1000 psia of helium to check for leaks using a thermal conductivity detector. The reactor was then depressurized to 25 psia of helium and placed in an electric heater. The helium placed in the headspace of the reactors was used as an internal standard for gas analysis. The temperatures were controlled and monitored within a standard error less than ± 0.5 °C by two calibrated J-type thermocouples in the thermal well of the reactor, which is directly connected to a digital thermometer. The reactors were weighed before and after the experiments to confirm that no leaks occurred. Minor losses (< 1 g) are a result of volatilization of portions of the anti-seize used on the bolt threads of the reactor head assemblage. At the end of experiments, final pressures and temperatures were recorded after the reactors cooled down to room temperatures. More details on the experimental protocol are given in Lewan (1993a, 1997).

Two types of HP experiments were conducted for a total of 25 experiments: (1) temperature series, and (2) time series. First, the experiments were performed under isothermal conditions for 72 h at 12 different temperatures (280, 300, 310, 320, 325, 330, 340, 345, 350, 355, 360 and 365 °C) to simulate the full range of petroleum generation from early bitumen generation to maximum oil generation. The second series consists of isothermal experiments conducted at variable times between 12 h and 132 h at four temperatures (310, 325, 340 and 355 °C), which were chosen based on the results obtained in the 72 h experiments in the temperature series experiments.

The experimental conditions employed in this investigation were selected based on the results of previous HP experiments to simulate expelled oil and associated primary gas generation (Ruble, 1996; Ruble et al., 2001; Lewan and Ruble, 2002; Lewan et al., 2006). Consequently, high maturity thermal cracking processes that reflect cracking of hydrocarbons (i.e., saturated and aromatic) to gas were negligible under the chosen conditions.

According to Lewan et al. (1979) and Lewan and Ruble (2002), if the rock is an oil prone source rock and the appropriate experimental time and temperature are employed, generated and expelled oil will accumulate on the water surface within the reactor. As previously described by those authors, this oil is physically, chemically and isotopically similar to natural crude oils.

2.3. Collection and quantification of generated products (mass balance)

The generated products were collected in the following order: headspace gas, expelled immiscible oil and recovered rock (with bitumen and residual kerogen). For the mass balance calculations, product yields generated in each experiment were quantified in milligrams and then reported in relation to the mass of original organic content as expressed in mg/g TOC_o. Table 2 gives the mass of original organic content used in these calculations for each experiment.

The headspace gas was collected in two evacuated 50 cm^3 stainless steel cylinders. Total moles of generated gas was calculated

using the ideal gas law with the recorded volume, temperature and pressure at the end of the experiment. The mole percentage of each component determined by the gas chromatography analysis was used to calculate its number of moles based on total moles generated. The amount in grams (or milligrams) of each gas generated was calculated from the number of moles multiplied by its molecular mass.

Following the same procedure described by Lewan (1993a, 1997), the expelled immiscible oil was quantitatively removed from the water surface in the reactor with a Pasteur pipette and a benzene rinse of the equipment. During the benzene rinse, only the portions of the reactor above the water were rinsed to collect all of the expelled oil. Expelled oil remaining in the pipette and collection funnel was also collected with the benzene rinse. During rinse process, evaporative losses occur mainly in the volatile fraction. The total mass of expelled oil is the sum of immiscible oil recovered by the pipette and benzene rinse.

The recovered rock was collected at the bottom of the reactor and submitted to air drying in a fume hood for several hours before a final recovered weight was recorded. Bitumen was extracted from dried aliquots of the recovered rock (3–30 g) using a Soxhlet apparatus with dichloromethane (DCM) as a solvent for about 24 h or until solvent in the siphon tube was clear. The recovered bitumen was filtered and the total weight was measured after solvent evaporation. For each experiment, the recovered bitumen was calculated on the basis of mg/g TOC_o using the recovered rock weight.

The residual kerogen was also quantified on the basis of mg/g TOC_o using the amounts of recovered rock, extracted bitumen and TOC of the extracted recovered rock for each experiment (Tables 3 and 4).

2.4. Analytical procedures of generated products

The recovered rocks were submitted to TOC and RE analyses to determine the remaining organic content and RE parameters for each experiment, as well as to petrographic analysis for vitrinite reflectance (%R_o; Table 4). Isolated kerogens from recovered rocks were submitted to elementary analysis for C, H, N, S_{total}, O, and Fe determinations. Aliquots of recovered rocks were extracted with organic solvent to remove the bitumen before petrographic analysis and kerogen isolation. The analytical procedures were the same used in the geochemical characterization of original rock and its isolated kerogen as described previously in Section 2.1.

The expelled oils recovered in each experiment were characterized by their bulk properties (density, API gravity, sulfur content and SARA petroleum fractions) and molecular composition (Tables 5 and 6).

Density was measured in an Anton Parr DMA 4500 Density Meter using the oscillating U-tube method and a mineral oil as with a known density as a standard. About 2 ml of sample were injected with a plastic 3 ml syringe into the U-tube making sure that no air bubbles were trapped. Before each run, the air density was checked to ensure that the U-tube is clean. The cleaning was done three times with chloroform and the remaining chloroform was removed from the U-tube with dry air from a pump. The density measurements were given at 60 F (15.56 °C) and the API gravity was calculated based on the formula: API gravity = (141.5/density)–131.5.

The sulfur analysis was performed with a Thermo Scientific FLASH 2000 Organic Elemental Analyzer (OEA-CHNS/O) using about 2 mg of sample and a Lube Oil as standard reference with a known percentage of sulfur.

The GC amenable portion of expelled oils was determined by Hewlett–Packard 6890 gas chromatograph equipped with a splitless injector and a flame ionization detector (GC-FID).

SARA fractions (saturates, aromatics, resins and asphaltenes) of the C_{15+} portion of the bitumen and oils were separated by column chromatography using an optimal sample weight of 50–100 mg according to the Standard Operating Procedure (SOP) used by the USGS labs. First, the procedure consists of asphaltene (ASPH) precipitation directly from the oil with *iso*-octane. The remaining maltene fraction was removed from the precipitate using a filtered Pasteur pipette (0.45 μm) to take up any residue and then transferred to a 7 ml vial. The maltenes were separated in a liquid chromatographic column, packed with silica gel grade 923 (100–200 mesh; 3 ml), silica gel grade 62 (60–200 mesh; 2 ml) and alumina (80–200 mesh; 1 ml). The maltenes dissolved in *iso*-octane were added on the top of the column to elute the saturated hydrocarbon fraction (SAT). Thereafter, the aromatic hydrocarbon fraction (ARO) was eluted using benzene as solvent. The final elution used a benzene/methanol (60/40 w/w) solvent to recover the resin fraction (RES). The solvent evaporation was performed in a fume hood for few days. The net weight of each fraction was calculated by the difference between the gross weight with the weight of empty vial. The RES and ASPH fractions are collectively referred to as polars, which are considered to be non-hydrocarbons. The percentages in weight of the C_{15+} fractions of SAT, ARO, RES and ASPH were normalized with the volatile fraction (C_6–C_{14} SAT and ARO) determined by quantitative GC performed in the Geochemistry Labs at Petrobras-CENPES. The experimental procedure of quantitative GC consisted in the separation of maltene fraction directly from whole oil using *n*-pentane (*n*-C_5) with sodium sulfate (Na_2SO_4). A known concentration of an internal standard (squalane, $C_{30}H_{62}$) is added to the solution for the quantification of the compounds, followed by mixing and leaving rest for 12 h. The maltene fraction (C_6–C_{35}) is separated from the heavier compounds (C_{35+}), which were precipitated in the bottom of the flask. Maltenes were analyzed in a Hewlett–Packard 6890 gas chromatograph equipped with a split/splitless injector and a flame ionization detector (GC-FID). The percentage by weight of the slices bounded by *n*-paraffins in the chromatogram is determined based on the integrated peak area of squalane in relation to its concentration in the whole oil.

Gas molecular composition (C_1–C_6 hydrocarbons, H_2S, CO_2, CO, O_2, H_2, N_2, He and Ar) was characterized by using a Hewlett–Packard 6890 gas chromatograph modified by Wasson Ece Instrumentation with a set of columns and three detectors (two thermal conductivity detectors, TCD, and one flame ionization detector, FID). The mole percentage of each component determined by this analysis was converted to moles using the ideal gas law with the recorded collection volumes, pressures and temperatures. The amount of each gas generated was reported in μmole/g TOC_o and exclude the He placed in the reactor as an internal standard (Tables 7 and 8). It should be noted that these reported gas compositions only represent head space gas and do not include the high concentrations of aqueous CO_2 that has been shown to be dissolved in HP waters (Lewan, 1997).

2.5. Transformation ratio calculation

Traditionally, the organic matter conversion to petroleum is represented by the transformation ratio (TR), which is a function of thermal maturity. TR is related to the fraction of the labile kerogen that has converted to petroleum. There are many ways to calculate TR using the decomposition of reactants or the formation of products.

The most common approach used by the petroleum industry was proposed by Tissot and Welte (1984) and Bordenave et al. (1993) that consider the decomposition of reactants based on the relationship between the original and residual petroleum generation potentials given by the S_2 peak of Rock–Eval pyrolysis

according to the equation: TR S_2 (%) = [($S_{2original} - S_{2residual}$)/($S_{2original}$)] * 100. In this calculation, the increase of TR (or decrease of S_2) is associated with bitumen, oil and gas generation. Table 4 shows the TR calculation using the traditional approach.

However, in this work, we adopt a different method considering just the expelled petroleum products (oil + HC gas) in order to examine the changes in their geochemical properties with increasing thermal maturity until the maximum yield is reached. It should be noted that this TR is dominated by expelled oil generation and therefore, represents the oil window with a TR of 100% denoting the end of oil generation associated with only part of the primary gas generation. The transformation ratio of each experiment was calculated as (100 * {[oil + HC gas yields]/maximum yield of expelled products} using a maximum yield of 728.23 mg/g TOC_o at 360 °C for 72 h as shown in Table 3 with product yields for each experiment.

2.6. Gas/oil ratio calculation

The quantity of oil and primary gas generated by hydrous pyrolysis allows calculation of GOR for each experiment and its behavior with the increase of transformation ratios (Table 9).

A mass GOR calculation (w/w) in Standard International Unit was obtained by dividing the yields of hydrocarbon gases and the yields of expelled oil in grams or mg/g TOC_o.

The volume GOR (v/v) as Oil-Field Unit was determined according the following procedure.

First the hydrocarbon (HC) gas volume is calculated with the ideal gas equation using room conditions and the total moles of HC gas (n_{HC}) generated (i.e., $n_{HC} = \sum C_1–C_5$).

The number of moles of each HC gas was determined from its mole percentage given by GC analysis multiplied by the number of moles of total gas (n_{total}) at the end of each experiment. The n_{total} was calculated by the ideal gas law: $n_{total} = (PV)/(RT)$, where P is the measured cool down pressure, T is the measured cool down temperature, V is the head space gas volume and R is the ideal gas constant.

The volume of hydrocarbon gas (V_{HC}) given in cm^3, assuming that these gases behaved ideally at room temperatures, was determined for each experiment following the equation:

V_{HC} (cm^3) = (n_{HC} RT)/P, where P is 14.7 psia, T is 288.71 K, n_{HC} is the sum of $C_1–C_5$ and R is 1.206,00 (cm^3 psi)/(mol K).

Secondly, the oil volume (V_{oil}) of each experiment in cm^3, was obtained by dividing the total mass of expelled oil in grams (m_{oil}) by its density (d_{oil}) in grams per cm^3 (V_{oil} [cm^3] = [m_{oil}]/[d_{oil}]).

It was not possible to measure the density of the oils generated in the experiments at 280 °C and 300 °C for 72 h due to insufficient amounts of expelled oil. In this case, a density of 0.864 g/cm^3 was used in the calculations, based on the average of density measured in expelled oils generated at the next lowest experimental temperatures (i.e., 310 °C and 320 °C).

Finally, the volumetric GOR (cm^3/cm^3 or m^3/m^3) was calculated by dividing the volume of HC gas by the volume of oil of each hydrous pyrolysis experiment: GOR (cm^3/cm^3) = V_{HC} (cm^3)/V_{oil}

Table 3
Product yields (kerogen, bitumen, oil and gas) and transformation ratio obtained for each hydrous pyrolysis experiment.

Temperature (°C)	Time (h)	Kerogen	Bitumen	Expelled oil	Total gas	HC gas	Total expelled (oil + HC gas)	% TR
Temperature series								
Unheated	0	**1333.33**	78.50	0	0	0	0	0
280	72	690.33	407.60	6.65	40.92	4.98	11.63	1.6
300	72	452.63	534.74	25.94	49.99	10.31	36.24	5.0
310	72	271.87	724.24	58.61	63.39	14.78	73.40	10.1
320	72	218.73	**844.84**	122.14	76.41	21.04	143.18	19.7
325	72	184.24	816.58	171.17	87.67	24.20	195.37	26.8
330	72	205.67	768.14	229.53	104.38	30.06	259.60	35.6
340	72	260.84	492.31	355.87	123.94	38.91	394.78	54.2
345	72	296.88	409.90	467.26	140.16	45.93	513.18	70.5
350	72	275.02	298.92	521.49	135.92	47.76	569.25	78.2
355	72	282.69	265.28	543.34	146.20	52.71	596.05	81.8
360	72	324.54	187.87	**662.17**	165.78	66.06	**728.23**	100.0
365	72	320.80	148.70	632.17	**184.75**	**76.98**	709.15	NA
Time series								
310	36	582.31	675.82	46.40	58.99	12.66	59.06	8.1
	72	354.06	724.24	58.61	63.39	14.78	73.40	10.1
	104	288.74	771.00	79.21	68.48	17.78	96.99	13.3
	132	286.83	686.96	109.50	73.03	19.17	128.67	17.7
325	24	264.62	796.25	82.62	71.51	15.90	98.53	13.5
	48	232.27	828.01	133.52	77.94	20.66	154.18	21.2
	72	252.76	816.58	171.17	87.67	24.20	195.37	26.8
	104	190.43	620.34	185.20	88.35	27.20	212.40	29.2
	120	141.59	649.27	219.49	97.19	28.77	248.26	34.1
340	24	291.59	538.59	199.95	93.55	24.80	224.75	30.9
	48	228.06	586.15	273.19	106.39	32.16	305.35	41.9
	72	308.60	492.31	355.87	123.94	38.91	394.78	54.2
	96	325.71	474.28	389.79	123.12	42.43	432.22	59.4
355	12	200.71	663.54	275.34	93.46	26.47	301.81	41.4
	30	281.87	473.22	410.51	119.46	38.30	448.81	61.6
	48	270.63	414.75	458.77	132.81	45.41	504.18	69.2
	72	314.63	265.28	543.34	146.20	52.71	596.05	81.8

Product yields in mg/g TOC_o; % TR = percentage of transformation ratio based on the expelled products given by the formula (oil + HC gas yields/total maximum yield of expelled products at 360 °C/72 h) * 100.
Maximum yields in bold print; NA = not applicable.

Table 4
Organic geochemical parameters of the recovered rocks and isolated kerogen for each hydrous pyrolysis experiment.

Temperature (°C)	Time (h)	TOC_R (wt%)	Extracted rock (g)	TOC_E (wt%)	S_1[a]	S_2[a]	S_3[a]	HI[a]	OI[a]	$S_1/TOC_o * 100$[a]	T_{max}[a]	PI (%)[a]	$\%R_o$	nR_o	H/C	O/C	% TRS_2
Temperature series																	
280	72	30.6	129.1	24.6	22.2	266.7	1.5	871.7	4.5	71.2	426	8	0.44	10	1.29	0.06	4.9
300	72	29.3	124.4	17.9	36.4	225.4	0.7	769.2	2.7	111.7	427	14	0.47	14	1.21	0.06	16.1
310	72	28.0	107.5	11.6	41.0	196.2	0.8	700.6	3.0	133.1	430	17	0.52	22	1.14	0.06	20.3
320	72	27.3	95.4	10.0	51.2	177.1	0.6	647.8	2.2	173.6	429	22	0.58	20	1.08	0.07	30.6
325	72	25.8	91.9	8.6	55.0	160.5	0.8	622.0	3.2	190.3	432	26	0.71	31	1.02	0.06	38.7
330	72	23.3	92.2	9.1	48.9	127.8	0.5	548.7	2.1	177.8	432	28	0.75	32	0.90	0.06	50.6
340	72	20.0	95.8	11.2	45.9	85.2	0.7	425.9	3.3	163.7	432	35	0.81	31	0.83	0.07	66.1
345	72	19.2	96.9	11.7	43.7	69.3	0.9	361.0	4.3	170.7	433	39	0.83	27	0.76	0.07	69.4
350	72	19.0	94.7	12.2	38.5	56.6	0.6	297.8	3.7	136.0	435	40	0.86	30	0.69	0.07	77.8
355	72	17.0	94.7	12.4	32.9	46.2	0.6	271.8	3.5	117.1	435	42	1.08	42	0.69	0.08	80.8
360	72	14.9	92.0	14.0	24.3	24.9	0.6	167.0	3.9	90.3	440	49	1.08	35	0.63	0.08	89.7
365	72	15.3	95.9	13.7	19.4	18.1	0.5	118.5	3.4	71.9	437	52	1.13	23	0.59	0.08	92.5
Time series																	
310	36	28.6	139.8	17.4	36.9	236.1	1.0	825.8	3.6	130.4	429	14	0.51	25	1.22	0.06	11.2
	72	28.0	140.0	11.6	41.0	196.2	0.8	700.6	3.0	133.1	430	17	0.52	22	1.14	0.06	20.3
	104	27.6	132.5	9.2	46.3	193.7	1.1	701.7	4.7	163.0	430	19	0.54	20	1.10	0.06	25.8
	132	27.9	130.2	9.3	44.2	188.9	0.9	676.2	3.3	155.6	429	19	0.57	25	1.11	0.06	29.7
325	24	25.5	135.9	8.5	43.1	178.9	0.6	701.8	2.3	150.7	430	19	0.70	40	1.15	0.07	19.4
	48	26.8	133.6	7.6	46.4	186.0	0.6	694.0	2.4	162.2	431	20	0.74	28	1.09	0.07	29.4
	72	25.8	126.1	8.6	55.0	160.5	0.8	622.0	3.2	190.3	432	26	0.71	31	1.02	0.06	38.7
	104	23.2	124.3	6.7	39.9	136.4	0.8	587.4	3.5	135.7	432	23	0.74	15	0.94	0.08	47.8
	120	24.2	126.1	5.0	48.1	120.6	0.7	498.5	2.8	164.7	433	29	0.75	17	0.91	0.07	53.1
340	24	24.2	123.0	9.7	46.5	161.0	0.8	665.2	3.4	168.5	430	22	0.80	44	0.87	0.08	36.2
	48	22.5	119.3	7.9	44.7	116.3	1.0	516.3	4.8	163.1	429	28	0.69	24	1.01	0.09	53.6
	72	20.0	113.3	11.2	45.9	85.2	0.7	425.9	3.3	165.1	432	35	0.81	31	0.83	0.07	66.1
	96	19.5	111.2	11.9	38.4	74.0	0.7	380.1	3.6	139.1	435	34	0.75	28	0.78	0.08	70.9
355	12	23.6	124.9	7.0	49.1	131.6	0.8	557.8	3.8	172.3	430	27	0.72	21	0.96	0.08	49.1
	30	20.3	114.7	10.5	47.2	91.3	0.8	449.8	3.7	166.2	435	34	0.74	24	0.83	0.08	65.1
	48	20.7	107.4	10.6	43.1	68.5	0.6	330.8	3.4	152.3	437	39	0.79	25	0.77	0.09	74.1
	72	17.0	105.4	12.4	32.9	46.2	0.6	271.8	3.5	117.1	434	42	1.08	42	0.69	0.08	80.8

TOC_R = residual organic carbon of recovered rock in weight percentage; TOC_E = residual organic carbon of extracted recovered rock in weight percentage; extracted rock = weight of extracted recovered rock (in g).

[a] Rock–Eval pyrolysis: S_1 = free volatile hydrocarbons (in mg/g rock), S_2 = residual petroleum generation potential (in mg/g rock), S_3 = CO_2 from organic source (in mg/g rock), HI = hydrogen index (S_2 * 100/TOC; in mg S_2/g TOC), OI = oxygen index (S_3 * 100/TOC; in mg S_3/g TOC), T_{max} = maximum temperature at S_2 peak (in °C), PI = production index ($S_1/S_1 + S_2r$); $\%R_o$ = mean random vitrinite reflectance in percent; nR_o = number of vitrinite reflectance measurements; H/C = atomic ratio of hydrogen to carbon in the kerogen; O/C = atomic ratio of oxygen to carbon in the kerogen; TRS_2 = transformation ratio based on the reduction of reactant given by the formula $[(S_{2original} - S_{2residual})/(S_{2original})] * 100$.

(cm^3). GOR was also converted in standard cubic feet (scf)/barrel (bbl), multiplying by a factor of 5.615 (Table 9).

2.7. Comparison with natural petroleum

A direct comparison between natural oils and those artificially generated requires great caution, because the geochemical parameters obtained by pyrolysis experiments may not be representative of those found in natural conditions. The correlation is hampered by the complexities inherent to the processes associated with the petroleum secondary alteration and the variability of organic facies favoring the mixing of fluids with different physicochemical characteristics.

To minimize the differences in organic facies, comparisons should be made ideally with oils generated by Batateira Beds in the Araripe Basin (NE-Brazil). However, these lacustrine beds have not reached sufficient thermal maturities for petroleum generation. As a result, this work used non-biodegraded petroleum generated from Lower Cretaceous lacustrine sequences of Brazilian sedimentary basins in an attempt to correlate with the petroleum generated by hydrous pyrolysis from a similar lacustrine source rock. The comparisons integrate physicochemical parameters as API gravity, sulfur content, GOR, percentages of petroleum fractions and molecular ratios of oil and gas components.

3. Results and discussion

3.1. Product yields and transformation ratios

The quantitative yields in mg/g TOC_o of the hydrous pyrolysis products as residual kerogen, bitumen, expelled immiscible oil, total and HC gases obtained from each experiment are shown in Table 3.

Based on the yields for temperature series experiments at 72 h (Table 3 and Fig. 2a), kerogen yields decrease significantly as bitumen yields increase during low pyrolysis temperatures, indicative of the bitumen generation stage related to the decomposition of kerogen. However, kerogen yields increase slightly at high pyrolysis temperatures (330–365 °C) due to the pyrobitumen formation (insoluble bitumen or inert carbon) through cross linking during oil formation. This cross-linking reaction parallels the thermal cracking reactions in various proportionalities depending on the pyrolysis method and has been observed and discussed in other HP and anhydrous experiments (Lewan et al., 1995) and has been observed in natural maturation of the Bakken Shale in the Williston Basin (Muscio and Horsfield, 1996). It should be noted that differentiating insoluble pyrobitumen from maturing kerogen is not feasible, so the residual organic carbon in the extracted recovered rocks includes both, which represent an organic hydrogen poor solid residue. So the increase of TOC in the extracted

Table 5
Bulk geochemical properties of expelled oils generated by hydrous pyrolysis and chemical compositions of oils and bitumens as a function of transformation ratio.

Temp. (°C)	Time (h)	API Gravity	Density (g/cm³)	%Sulfur	%C_{6-14}	%SAT		%ARO		%RES		%ASPH		%POLARS		% TR
						Oil	Bit.	Oil	Bit.	Oil	Bit.	Oil	Bit.	Oil	Bit.	
Temperature series																
Unheated	NA	NA	NA	NA	NA	NA	14.5	NA	23.0	NA	41.5	NA	21.0	NA	62.5	0
280	72	ND	ND	1.55	ND	37.9	6.6	30.4	15.6	26.5	26.8	5.2	51.0	31.7	77.8	1.6
300	72	ND	ND	1.41	27.8	29.8	6.7	21.8	16.5	16.8	18.6	3.8	58.2	20.7	76.7	5.0
310	72	31.87	0.866	1.22	17.8	37.8	7.1	25.1	16.9	15.2	15.3	4.0	60.8	19.2	76.1	10.1
320	72	30.27	0.875	1.23	24.9	35.3	6.8	21.1	15.0	14.0	10.1	4.8	68.0	18.7	78.2	19.7
325	72	30.17	0.875	1.12	16.2	39.6	8.2	23.5	17.3	16.4	10.6	4.2	63.9	20.6	74.5	26.8
330	72	30.41	0.874	1.04	16.3	34.9	9.4	29.1	18.5	15.7	11.3	4.0	60.8	19.7	72.1	35.6
340	72	29.23	0.880	0.87	17.8	34.2	13.5	27.3	23.1	15.6	11.4	5.1	52.1	20.7	63.4	54.2
345	72	29.00	0.882	0.99	24.1	31.1	16.1	26.6	26.1	13.0	13.9	5.1	43.9	18.1	57.8	70.5
350	72	28.08	0.887	0.90	23.7	30.0	16.7	26.3	30.0	14.1	17.6	5.8	35.8	20.0	53.4	78.2
355	72	28.61	0.884	0.96	24.6	30.0	18.7	25.6	26.0	13.0	13.8	6.7	41.5	19.7	55.3	81.8
360	72	26.53	0.895	0.92	25.4	27.2	13.7	27.2	24.3	12.8	15.7	7.4	46.4	20.3	62.0	100.0
365	72	29.85	0.877	0.90	28.2	28.9	12.0	24.4	29.8	12.6	18.5	6.0	39.7	18.5	58.2	NA
Time series																
310	36	31.33	0.869	1.42	20.0	38.7	6.3	21.0	15.2	15.6	18.6	4.7	60.0	20.3	78.5	8.1
	72	31.87	0.866	1.22	17.8	37.8	7.1	25.1	16.9	15.2	15.3	4.0	60.8	19.2	76.1	10.1
	104	31.60	0.868	1.20	20.1	36.7	7.0	22.0	14.9	15.7	14.3	5.5	63.8	21.2	78.1	13.3
	132	31.13	0.870	1.21	18.8	38.3	7.3	23.2	14.7	15.9	9.7	3.8	68.3	19.7	78.0	17.7
325	24	30.12	0.876	1.37	17.9	36.3	5.0	25.3	13.4	16.3	11.6	4.2	69.9	20.5	81.6	13.5
	48	29.53	0.879	1.20	16.2	34.6	6.6	27.5	15.2	17.1	10.3	4.6	68.0	21.7	78.2	21.2
	72	30.17	0.875	1.12	16.2	39.6	8.2	23.5	17.3	16.4	10.6	4.2	63.9	20.6	74.5	26.8
	104	31.15	0.870	0.93	20.0	34.8	9.6	26.9	19.0	15.0	10.3	3.3	61.1	18.3	71.4	29.2
	120	30.52	0.873	1.04	18.9	35.7	10.3	26.5	16.9	15.5	9.0	3.3	63.8	18.8	72.8	34.1
340	24	26.79	0.894	1.24	14.3	34.4	7.5	28.0	16.0	19.7	8.6	3.6	67.9	23.3	76.5	30.9
	48	28.67	0.883	0.99	16.4	34.3	12.1	26.8	22.4	16.9	15.8	5.6	49.6	22.5	65.5	41.9
	72	29.23	0.880	0.87	17.8	34.2	13.5	27.3	23.1	15.6	11.4	5.1	52.1	20.7	63.4	54.2
	96	29.87	0.877	0.82	24.1	31.4	14.9	26.3	24.2	14.5	12.0	3.7	48.9	18.2	60.9	59.4
355	12	21.97	0.922	1.29	13.0	24.9	7.1	28.6	15.4	18.7	9.9	14.9	67.6	33.5	77.5	41.4
	30	24.80	0.905	1.17	21.4	26.7	12.2	27.1	20.6	15.3	11.5	9.5	55.7	24.8	67.2	61.6
	48	26.93	0.893	1.01	23.8	27.3	14.5	26.1	25.1	15.3	14.6	7.5	45.7	22.8	60.4	69.2
	72	28.61	0.884	0.96	24.6	30.0	18.7	25.6	26.0	13.0	13.8	6.7	41.5	19.7	55.3	81.8

%SAT = percentage of C_{15+} saturates, %ARO = percentage of C_{15+} aromatics, %RES = percentage of resins, %ASPH = percentage of asphaltenes; %POLARS = %RES + %ASPH; Bit. = Bitumen.
%C_6–C_{14} = percentage of volatile fraction of the saturated and aromatic hydrocarbons. Percentages of expelled oils are normalized with volatile fraction; NA = not applicable; ND = not determined.

recovered rocks (Table 4) is directly related to the pyrobitumen formation at higher pyrolysis temperatures (330–365 °C), reflecting in the increase of kerogen yields as observed in Figs. 2 and 3.

The maximum bitumen yield occurs at 320 °C after 72 h. Subsequently, the bitumen yields progressively decrease at higher temperatures. Oil generation and expulsion starts very slowly and only increases significantly after more severe thermal conditions than the experiment at 320 °C for 72 h, characterizing the oil generation stage related to the decomposition of bitumen. The maximum yield of expelled oil (662 mg/g TOC_o) is attained at 360 °C for 72 h. This behavior strongly supports a product–precursor relationship between immiscible oil and bitumen phases (Lewan, 1994). At higher thermal maturities, the oil yield decreases slightly, suggesting the beginning of post-oil generation at 365 °C/72 h, which is probably related to some oil decomposition (i.e., cracking of hydrocarbons to secondary gas generation and crosslinking to pyrobitumen; Fig. 2a).

Time series experiments under isothermal conditions also corroborate these interpretations (Fig. 2b). The bitumen yields are higher in isothermal experiments at low temperatures (310 °C and 325 °C) and decrease gradually at higher temperatures (340 °C and 355 °C) associated with longer times. From the 325 °C experiment at 72 h, the bitumen yields generally show a significant decrease, indicating the beginning of oil generation from bitumen decomposition.

Total gas generation gradually increases with increasing thermal maturation as indicated by higher temperatures, but there are no abrupt changes during the bitumen and oil generation stages (Fig. 2). The differences between headspace (total gas) and HC gases can be attributed mainly to significant CO_2 generation (Table 3). The HC gas yield at the maximum oil yield is 66 mg HC/g TOC_o, which corresponds to only 9% of the sum of oil and HC gas. The HC gas yields keep increasing after the oil generation stage as a result of the decomposition of bitumen at higher thermal maturities and minor oil cracking at 365 °C for 72 h (Fig. 2a). It is important to mention that the residual bitumen retained in the source rock at the end of oil generation stage (360 °C/72 h) represents 22% of the maximum bitumen generated, and can contribute as a possible source for liquid hydrocarbons (condensate) and continued primary gas generation at higher thermal maturities (Table 3).

Fig. 3 shows the behavior of product yields as a function of the transformation ratios (TR). At maximum bitumen generation, TR reaches a value of 20–25% (bitumen zone), after which expelled oil yields significantly increase until 100% TR at the end of the oil generation (oil zone).

The quantitative results of hydrous pyrolysis products obtained in this work reinforces that oil generation is a two-step process in which most expelled hydrocarbon rich oil is formed from the bitumen decomposition (Franks and Goodier, 1922; Allred, 1966; Tissot, 1969; Tissot and Espitalié, 1975; Lewan, 1985, 1993a, 1994; Baskin and Peters, 1992; Ruble et al., 2001; Behar et al., 2008, 2010). This two-step process (kerogen → bitumen → oil) was first recognized in oil shale retorting by Engler (1913).

Table 6
Gas chromatography derived compositional parameters of expelled oils and bitumens produced by hydrous pyrolysis of a Type I kerogen.

Temp. (°C)	Time (h)	API gravity	% TR	%*n*-alkanes/total area		pristane/phytane		pristane/*n*-C_{17}		phytane/*n*-C_{18}		CPI		%*n*-C_6–C_{35}
				Oil	Bit.	Oil	Bit.	Oil	Bit.	Oil	Bit.	Oil	Bit.	
Temperature series														
Unheated	NA	NA	0	NA	4.45	NA	0.34	NA	2.77	NA	3.41	NA	4.17	NA
280	72	ND	1.6	22.6	6.12	1.59	1.32	2.69	2.73	3.40	2.59	0.73	1.66	ND
300	72	ND	5.0	20.9	6.50	1.90	1.47	2.51	2.33	2.31	2.17	0.95	1.34	9.4
310	72	31.87	10.1	17.6	7.80	1.92	1.41	2.12	1.93	1.81	1.74	0.97	1.12	8.5
320	72	30.27	19.7	17.4	7.29	1.81	1.24	1.76	1.71	1.40	1.59	1.06	1.20	9.3
325	72	30.17	26.8	18.4	8.87	1.86	1.28	1.55	1.47	1.22	1.32	1.00	1.15	5.8
330	72	30.41	35.6	16.9	9.74	1.61	1.29	1.31	1.34	1.10	1.18	1.00	1.11	5.8
340	72	29.23	54.2	16.4	11.42	1.73	1.36	1.03	1.07	0.81	0.94	0.98	1.08	7.1
345	72	29.00	70.5	16.3	11.52	1.66	1.32	0.90	0.97	0.71	0.82	1.05	1.05	10.7
350	72	28.08	78.2	16.2	12.04	1.61	1.24	0.76	0.84	0.60	0.77	1.04	1.00	10.6
355	72	28.61	81.8	16.3	13.29	1.65	1.17	0.70	0.75	0.54	0.65	1.04	1.02	11.0
360	72	26.53	100.0	19.3	8.48	1.85	1.17	0.52	0.46	0.37	0.36	1.01	1.08	11.5
365	72	29.85	NA	16.7	10.94	1.82	1.98	0.37	0.42	0.26	0.20	1.05	0.95	12.1
Time series														
310	36	31.33	8.1	19.1	5.90	1.88	1.45	2.48	2.64	2.16	2.59	1.01	1.45	ND
	72	31.87	10.1	17.6	7.80	1.92	1.41	2.12	1.93	1.81	1.74	0.97	1.12	8.5
	104	31.60	13.3	17.7	8.25	1.90	1.52	1.98	1.78	1.59	1.52	1.02	1.13	6.2
	132	31.13	17.7	18.1	8.92	1.90	1.53	1.82	1.72	1.52	1.46	0.99	1.18	6.3
325	24	30.12	13.5	17.0	8.86	1.94	1.43	2.20	2.00	1.86	1.77	0.97	1.16	4.9
	48	29.53	21.2	17.1	7.86	1.86	1.39	1.77	1.66	1.44	1.53	1.01	1.20	5.0
	72	30.17	26.8	18.4	8.87	1.86	1.28	1.55	1.47	1.22	1.32	1.00	1.15	5.8
	104	31.15	29.2	18.6	9.32	1.72	1.30	1.39	1.32	1.12	1.20	1.05	1.12	7.5
	120	30.52	34.1	17.4	10.31	1.61	1.32	1.26	1.27	1.06	1.15	1.00	1.09	7.3
340	24	26.79	30.9	15.6	9.38	1.71	1.39	1.53	1.49	1.27	1.36	1.00	1.19	4.0
	48	28.67	41.9	16.4	9.97	1.68	1.39	1.19	1.21	0.97	1.02	1.03	1.11	5.6
	72	29.23	54.2	16.4	11.42	1.73	1.36	1.03	1.07	0.81	0.94	0.98	1.08	7.1
	96	29.87	59.4	18.5	12.88	1.60	1.64	0.92	0.99	0.75	0.72	0.98	1.05	11.4
355	12	21.97	41.4	13.5	9.20	1.89	1.40	1.38	1.39	1.10	1.26	1.04	1.09	3.9
	30	24.80	61.6	14.4	11.61	1.64	1.39	0.98	1.06	0.81	0.92	0.99	1.06	8.2
	48	26.93	69.2	16.1	11.74	1.80	1.24	0.84	0.86	0.64	0.78	1.00	1.06	10.1
	72	28.61	81.8	16.3	13.29	1.65	1.17	0.70	0.75	0.54	0.65	1.04	1.02	11.0

%*n*-alkanes/total area = percentage of the sum of the area of *n*-alkanes identified/gas-chromatogram total area; Bit. = Bitumen. NA = not applicable; ND = not determined.
%*n*-C_6–C_{35} = percentage of *n*-alkanes (C_6–C_{35}) from whole oil given by quantitative-GC.
CPI (carbon preference index) $= \frac{1}{2}\left(\frac{C_{25}+C_{27}+C_{29}+C_{31}}{C_{24}+C_{26}+C_{28}+C_{30}+C_{32}} + \frac{C_{25}+C_{27}+C_{29}+C_{31}+C_{33}}{C_{24}+C_{26}+C_{28}+C_{30}+C_{32}}\right)$.

Table 7
Yields and molecular indices of gases generated by hydrous pyrolysis in the temperature series experiments for 72 h as a function of transformation ratio.

Yields (μmol/g TOC_o)	Temperature series (°C) for 72 h											
	280	300	310	320	325	330	340	345	350	355	360	365
Methane	112.6	228.7	341.5	489.3	566.0	732.0	949.2	1145.7	1188.3	1357.0	1723.1	2013.4
Ethane	22.7	55.2	95.3	150.3	182.9	243.0	321.8	383.6	391.2	435.5	526.6	609.9
Propane	13.0	31.3	53.0	77.8	93.6	120.5	156.4	183.2	190.3	213.5	256.2	318.4
iso-Butane	5.0	10.9	17.0	21.9	25.9	31.0	37.5	42.0	43.3	47.3	52.9	65.6
n-Butane	3.8	10.1	17.2	22.8	27.9	33.7	41.6	46.1	48.7	52.6	58.8	78.1
iso-Pentane	2.7	5.8	8.9	9.2	11.2	12.4	14.3	14.7	16.1	16.8	17.8	23.0
n-Pentane	3.4	6.0	8.9	8.3	10.2	10.8	12.5	12.1	13.6	13.1	14.3	18.4
$\sum C_1$–C_5	163.2	347.9	541.8	779.5	917.5	1183.4	1533.3	1827.3	1891.5	2135.9	2649.8	3126.8
∑unsHC	3.8	3.9	2.3	2.1	5.3	5.4	7.6	7.6	9.7	4.2	6.5	5.3
Carbon dioxide	732.3	825.1	1015.9	1169.7	1352.5	1590.3	1837.2	2036.8	1912.9	2026.0	2171.3	2352.8
Nitrogen	9.0	2.1	9.1	8.6	9.5	11.2	9.4	11.6	9.7	13.7	8.9	11.8
Hydrogen	36.9	67.5	102.2	133.7	145.8	171.7	199.8	223.2	224.3	211.4	212.8	189.1
Hydrogen sulfide	0.0	0.0	0.0	0.0	0.0	0.0	0.0	0.0	0.0	0.0	0.0	0.0
Molecular indices												
$[CO_2/(CO_2 + CH_4)] * 100$	86.68	78.30	74.84	70.51	70.50	68.48	65.93	64.00	61.68	59.89	55.75	53.89
$C_1/(C_2 + C_3 + C_4 + C_5)$	2.22	1.92	1.71	1.69	1.61	1.62	1.63	1.75	1.69	1.74	1.86	1.81
$C_1/(C_2 + C_3)$	3.16	2.65	2.30	2.15	2.05	2.01	1.99	2.02	2.04	2.09	2.20	2.17
C_1/C_2	4.96	4.15	3.58	3.26	3.10	3.01	2.95	2.99	3.04	3.12	3.27	3.30
C_2/C_3	1.75	1.76	1.80	1.93	1.95	2.02	2.06	2.09	2.06	2.04	2.06	1.92
C_3/C_4	1.47	1.49	1.55	1.74	1.74	1.86	1.98	2.08	2.07	2.14	2.29	2.21
i-C_4/n-C_4	1.33	1.08	0.99	0.96	0.93	0.92	0.90	0.91	0.89	0.90	0.90	0.84
i-C_5/n-C_5	0.79	0.97	1.00	1.11	1.10	1.14	1.14	1.21	1.18	1.28	1.25	1.25
C_2/i-C_4	4.50	5.06	5.61	6.86	7.05	7.84	8.57	9.13	9.03	9.20	9.96	9.29
$C_3/(C_4 + C_5)$	3.13	3.93	4.50	4.91	5.11	5.36	5.70	5.80	6.00	6.08	6.37	6.67
Transformation ratio (%)	1.6	5.0	10.1	19.7	26.8	35.6	54.2	70.5	78.2	81.8	100	NA

∑unsHC – unsaturated hydrocarbons = ethene + ethylene + propene + propylene + *trans*-2-butene + 1-butene + *iso*-butene + *cis*-2-butene. NA = not applicable.

Comparing these results with other hydrous pyrolysis studies using Type I kerogens such as the Green River Formation (Ruble, 1996; Ruble et al., 2001), show a notable difference in the temperature for 72 h at which maximum bitumen occurs. Maximum bitumen generation occurs at a lower temperature (320 °C/72 h; Table 3) than that reported for the Type I kerogen in the Green River Formation (325–330 °C/72 h, Ruble, 1996; Ruble et al., 2001). These differences may be attributed to the high amount of organic sulfur incorporated in the kerogen matrix, which has been shown to cause bitumen and oil generation at lower thermal maturities (Lewan, 1985, 1998; Orr, 1986; Baskin and Peters, 1992).

3.2. Thermal maturity indices

Thermal maturity was assessed based on organic geochemical parameters of the recovered rocks and isolated kerogen for each HP experiment as shown in Table 4.

The effect of increasing thermal maturation and consequent conversion of kerogen into petroleum was observed by decreasing TOC (Fig. 4a) and HI (Fig. 4b) of the recovered rocks, and also by the decrease of atomic H/C ratio of isolated kerogen (Fig. 4c). These geochemical parameters systematically decrease with increasing transformation ratios as a result of the hydrogen and carbon losses during the petroleum generation and expulsion. According to Jarvie (1991), the reduction of TOC with increasing maturation can be explained by the conversion of convertible carbon present in the kerogen (original or remaining potential) to extractable organic matter carbon (free hydrocarbons) associated with the expulsion of gaseous and liquid hydrocarbons from the source rock. This process can be observed indirectly from the increase of the free volatile hydrocarbons given by the S_1 peak of Rock–Eval pyrolysis. As shown in Table 4, changes in the S_1 peak may be monitored by its ratio with TOC_o and then multiplied by 100. In the initial stages of thermal maturation, this parameter increases to a value of 190.3 mg/g TOC_o at 325 °C for 72 h and then decreases to 71.9 mg/g TOC_o at 365 °C for 72 h, with only one outlier at 345 °C for 72 h. This trend is similar in part to that of the bitumen content (Table 3 and Fig. 2) with the exceptions of the bitumen maximum occurring at 320 °C for 72 h and decreasing bitumen values being significantly lower in relation to the values of $S_1/TOC_o \times 100$ (Table 4).

The maximum carbon loss for an immature Type I kerogen is 80% (maximum convertible carbon) as suggested by Jarvie (1991) and Bordenave et al. (1993). Under overmature conditions, at which stage kerogen is composed of a carbon rich residue, they suggest that no potential to generate oil or gas remains in the highly condensed hydrogen poor chemical structure.

In the HP maturation series, the maximum carbon loss reached 52% at the maximum yield of expelled oil (i.e., 360 °C/72 h). This value is < 70–80% as determined for Type I kerogens (Jarvie, 1991; Bordenave et al., 1993; Baskin, 1997), because the formation of pyrobitumen was not considered in their assumptions. The insoluble bitumen minimizes the carbon losses during petroleum generation and expulsion as the organic carbon increases in the solid residue of the source rock with increasing thermal maturity. The increase in TOC based on the original TOC is a common occurrence caused by pyrobitumen formation and has been observed in other HP experiments (Lewan et al., 1995) and in natural maturation of oil prone source rocks (Muscio and Horsfield, 1996).

Associated with carbon losses, a very rapid depletion of the hydrogen can be observed through the HI and kerogen atomic H/C ratio (Fig. 4b and c). It is important to note that the HI values are decreasing more than the increases in expelled oil and gas yields, which suggests that some of the HI is reduced by the formation of pyrobitumen.

Hydrocarbon generation can also be observed by the Rock–Eval production index (PI; Fig. 4d), which systematically increases with the increasing transformation ratio. The same behavior was obtained for maximum temperature of Rock–Eval pyrolysis (T_{max}; Fig. 4e) and vitrinite reflectance (%R_o; Fig. 4f) with increasing TR.

T_{max} shows a small increase from an initial value of 422 °C reaching up 440 °C at the maximum expelled oil yield. This narrow range of change in T_{max} was previously described by Espitalié

Table 8
Yields and molecular indices of gases generated by hydrous pyrolysis in the time series experiments as a function of transformation ratio.

Yields (μmol/g TOC_o)	310 °C				325 °C					340 °C				355 °C			
	36 h	72 h	104 h	132 h	24 h	48 h	72 h	104 h	120 h	24 h	48 h	72 h	96 h	12 h	30 h	48 h	72 h
Methane	286.6	341.5	413.3	461.0	358.6	483.6	566.0	647.9	682.0	568.5	757.7	949.2	1056.2	621.1	930.7	1093.9	1357.0
Ethane	71.3	95.3	118.2	136.1	103.4	149.6	182.9	211.5	227.9	189.3	257.1	321.8	351.2	202.7	310.2	360.5	435.5
Propane	40.3	53.0	64.8	73.4	55.8	77.6	93.6	106.9	114.7	95.8	127.0	156.4	168.1	101.5	150.3	176.0	213.5
iso-Butane	14.3	17.0	20.0	21.4	18.2	22.7	25.9	28.0	29.2	27.2	32.7	37.5	38.2	28.5	36.9	41.5	47.3
n-Butane	13.1	17.2	21.1	22.3	17.3	23.3	27.9	31.0	32.8	27.2	35.1	41.6	43.2	27.5	38.7	44.3	52.6
iso-Pentane	8.0	8.9	10.1	9.5	9.1	10.3	11.2	11.3	11.8	11.5	13.2	14.3	14.1	11.8	13.9	15.3	16.8
n-Pentane	8.0	8.9	10.1	8.7	8.3	9.4	10.2	11.0	10.7	9.8	11.3	12.5	12.3	9.0	11.3	12.4	13.1
$\sum C_1$–C_5	441.6	541.8	657.5	732.4	570.6	776.5	917.5	1047.7	1109.0	929.2	1234.2	1533.3	1683.1	1002.2	1492.1	1743.9	2135.9
∑unsHC	9.7	2.3	4.6	4.6	10.2	6.8	5.3	5.0	5.3	10.8	8.6	7.6	7.7	14.6	9.1	32.4	4.2
Carbon dioxide	960.1	1015.9	1060.1	1129.3	1171.0	1217.3	1352.5	1302.5	1469.1	1465.6	1593.7	1837.2	1737.1	1432.4	1750.6	1891.7	2026.0
Nitrogen	9.2	9.1	9.0	11.9	12.1	8.0	9.5	9.0	8.2	10.8	9.7	9.4	9.5	8.3	8.7	8.1	13.7
Hydrogen	93.4	102.2	106.4	117.4	114.4	131.9	145.8	148.9	158.8	167.6	181.2	199.8	218.5	168.3	208.6	211.2	211.4
Hydrogen sulfide	0.0	0.0	0.0	0.0	0.0	0.0	0.0	0.0	0.0	0.0	0.0	0.0	0.0	0.0	0.0	0.0	0.0
Molecular indices																	
$[CO_2/(CO_2 + CH_4)] * 100$	77.01	74.84	71.95	71.01	76.56	71.57	70.50	66.78	68.29	72.05	67.78	65.93	62.19	69.75	65.29	63.36	59.89
$C_1/(C_2 + C_3 + C_4 + C_5)$	1.85	1.71	1.69	1.70	1.69	1.65	1.61	1.62	1.60	1.58	1.59	1.63	1.68	1.63	1.66	1.68	1.74
$C_1/(C_2 + C_3)$	2.57	2.30	2.26	2.20	2.25	2.13	2.05	2.03	1.99	1.99	1.97	1.99	2.03	2.04	2.02	2.04	2.09
C_1/C_2	4.02	3.58	3.50	3.39	3.47	3.23	3.10	3.06	2.99	3.00	2.95	2.95	3.01	3.06	3.00	3.03	3.12
C_2/C_3	1.77	1.80	1.82	1.85	1.85	1.93	1.95	1.98	1.99	1.97	2.02	2.06	2.09	2.00	2.06	2.05	2.04
C_3/C_4	1.47	1.55	1.58	1.68	1.57	1.69	1.74	1.81	1.85	1.76	1.87	1.98	2.07	1.81	1.99	2.05	2.14
i-C_4/n-C_4	1.09	0.99	0.95	0.96	1.05	0.97	0.93	0.90	0.89	1.00	0.93	0.90	0.88	1.04	0.96	0.94	0.90
i-C_5/n-C_5	1.00	1.00	1.00	1.10	1.10	1.09	1.10	1.03	1.10	1.18	1.17	1.14	1.15	1.31	1.23	1.23	1.28
C_2/i-C_4	4.98	5.61	5.92	6.36	5.70	6.58	7.05	7.56	7.80	6.96	7.86	8.57	9.20	7.11	8.40	8.69	9.20
$C_3/(C_4 + C_5)$	4.01	4.50	4.76	4.84	4.35	4.88	5.11	5.42	5.49	4.93	5.41	5.70	5.93	4.95	5.54	5.75	6.08
Transformation ratio (%)	8.1	10.1	13.3	17.7	13.5	21.2	26.8	29.2	34.1	30.9	41.9	54.2	59.4	41.4	61.6	69.2	81.8

∑unsHC – unsaturated hydrocarbons = ethene + ethylene + propene + propylene + *Trans*-2-butene + 1-butene + *iso*-butene + *cis*-2-butene.

Table 9
Petroleum volumes and gas/oil ratios (GOR) obtained by hydrous pyrolysis for each experiment and theirs correlations with the transformation ratio.

Temperature (°C)	Time (h)	Number of moles ($n_{HC} = \sum C_1–C_5$)	Gas volume (cm^3)	Oil volume (cm^3)	GOR (kg/kg)	GOR (m^3/m^3)	GOR (scf/bbl)	% TR
Temperature series								
280	72	0.00750	177.75	0.35	0.75	508	2852	1.6
299	72	0.01711	405.36	1.48	0.40	274	1538	5.0
310	72	0.02485	588.52	3.12	0.25	189	1061	10.1
320	72	0.03401	805.55	6.13	0.17	131	736	19.7
325	72	0.03935	932.07	8.44	0.14	110	618	26.8
330	72	0.04826	1143.13	10.77	0.13	106	595	35.6
340	72	0.06304	1493.26	16.72	0.11	89	500	54.2
345	72	0.06975	1652.08	20.35	0.10	81	455	70.5
350	72	0.07949	1882.78	24.86	0.09	76	427	78.2
355	72	0.08871	2101.16	25.68	0.10	82	460	81.8
360	72	0.10521	2491.94	29.52	0.10	84	472	100.0
365	72	0.12807	3033.43	29.70	0.12	102	573	NA
Time series								
310	36	0.01845	436.92	2.24	0.27	195	1095	8.1
	72	0.02485	588.52	3.12	0.25	189	1061	10.1
	104	0.02777	657.69	3.88	0.22	170	954	13.3
	132	0.03091	732.16	5.34	0.18	137	769	17.7
325	24	0.02490	589.89	4.14	0.19	142	797	13.5
	48	0.03394	803.80	6.68	0.15	120	674	21.2
	72	0.03935	932.07	8.44	0.14	110	618	26.8
	104	0.04583	1085.59	9.37	0.15	116	651	29.2
	120	0.04938	1169.73	11.26	0.13	104	584	34.1
340	24	0.03803	900.83	9.21	0.12	98	550	30.9
	48	0.05099	1207.86	12.85	0.12	94	528	41.9
	72	0.06304	1493.26	16.72	0.11	89	500	54.2
	96	0.06838	1619.63	18.16	0.11	89	500	59.4
355	12	0.04373	1035.78	13.10	0.10	79	444	41.4
	30	0.06378	1510.59	19.49	0.09	78	438	61.6
	48	0.07339	1738.20	21.74	0.10	80	449	69.2
	72	0.08871	2101.16	25.68	0.10	82	460	81.8

scf = standard cubic feet; bbl = oil barrel.

(1986) and Bordenave et al. (1993) in natural maturation of Type I kerogen and in HP experiments on Green River source rocks with Type I kerogen (Huizinga et al., 1988; Ruble, 1996). The narrow range suggests that Type I kerogen as a more homogeneous chemical structure than that of Type II and III kerogen, which show greater ranges in T_{max} changes with thermal maturation. However, the range of T_{max} change in the Brazilian Type I kerogen (422–440 °C, 18 °C) is greater than that observed for the Green River Type I kerogen in HP experiments by Huizinga et al. (1988; 442–450 °C, 8 °C). In addition, the initial T_{max} of immature Brazilian Type I kerogen (422 °C) is notably lower than those reported for immature Green River Type I kerogen (438 °C, Ruble et al., 2001; and 448 °C, Huizinga et al., 1988). These differences suggest that the Brazilian Type I kerogen may be less homogenous in chemical structure and more labile to petroleum generation than the Green River Type I kerogen. Higher organic sulfur in the Brazilian Type I kerogen may account in part for these attributes.

Gradual changes in vitrinite reflectance (%R_o) appear to be suppressed showing similar trends as defined by Lewan (1985, 1993b). This type of vitrinite is suggested to be more hydrogen rich and shows a lower reflectance and possibly some weak fluorescence (Tissot et al., 1987). Considering the petroleum generation stages presented in Fig. 2a, the beginning of oil generation stage correlates with 0.58 %R_o (320 °C/72 h) and reaches 1.08 %R_o at the maximum oil yield (360 °C/72 h). The post-maximum oil yield reaches 1.13 %R_o (365 °C/72 h). These values are close to those defined by Tissot and Welte (1984) in the Uinta Basin for the same kerogen type, but are much lower than those reported by Ruble et al. (2001). However, the beginning of the oil zone occurs slightly late around 0.7 %R_o, but extends until 1.1 %R_o at the maximum or peak of the oil generation curve. These differences suggest that vitrinite reflectance is a good monitor of thermal stress experienced by a source rock, but because of differing kinetics for oil generation, it is not necessarily a good monitor of the extent of oil generation (Lewan, 1985; Tissot et al., 1987).

3.3. Gas/oil ratio

The petroleum volumes and gas/oil ratios (GOR in w/w or v/v) obtained by hydrous pyrolysis for each experiment are presented in Table 9.

The general trend of GOR with the increase of transformation ratio (TR) is shown in Fig. 5. The higher GOR values (130–500 m^3/m^3) at TR < 25% are due to the higher amounts of early gas generated relative to very low amounts of expelled oil. With the increase of transformation ratio, the GOR decreases curvilinearly to values around 80–90 m^3/m^3 and remain relatively constant until the maximum oil yield (360 °C/72 h) at a TR of 100%. This decrease is due to the higher proportion of expelled oil (6–10 times) compared to hydrocarbon gases ($C_1–C_5$) generated during the oil window at TR > 25%. No significant variations in the GOR occur at the higher TR values. This indicates that the amount primary gas generated during kerogen decomposition to bitumen and bitumen decomposition to oil is proportionally the same as the amount of generated oil in the oil zone.

GOR increases slightly to 102 m^3/m^3 in the post oil generation experiment at 365 °C/72 h (Table 9). This indicates that some secondary gas is beginning to form from the thermal cracking of the expelled oil on the water surface in the reactor.

In a comparative study, similar behavior of the GOR was reported by Lewan and Henry (2001) using hydrous pyrolysis experiments under analogous time–temperature conditions to those applied in this work. The curvilinear decrease of the GOR during the oil generation stage was observed in the different types

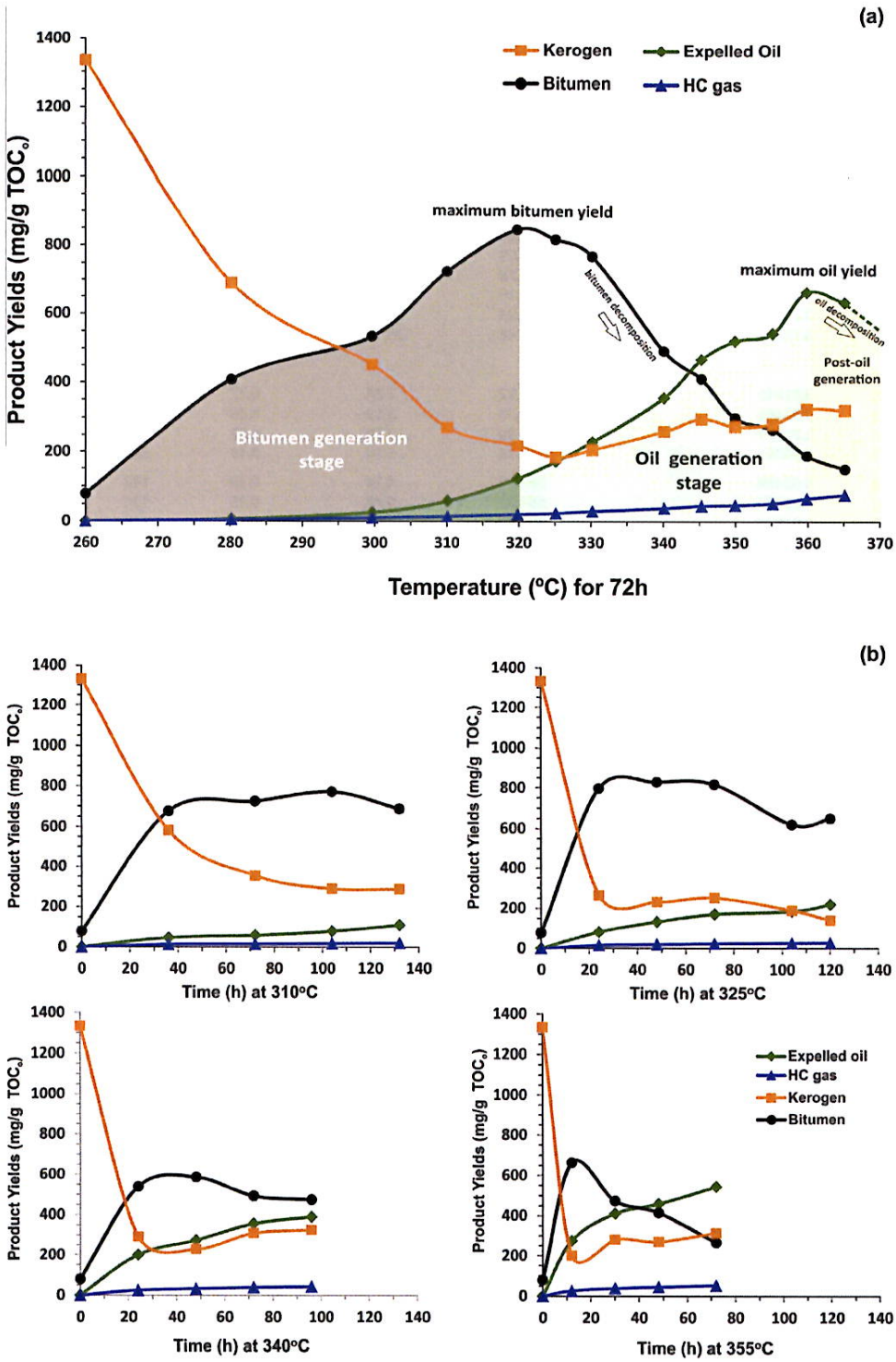

Fig. 2. Product yields generated by hydrous pyrolysis as a function of experimental conditions. (a) temperature series experiments for 72 h; (b) time series experiments at 310/325/340/355 °C.

of kerogen, but the Type III kerogen generated higher GOR than the others oil prone kerogens (Type I, II and IIS). However, despite the Type III kerogen be considered gas prone potential, it generates the lowest amounts of HC gas compared with oil prone kerogens (Hunt, 1996; Behar et al., 1997; Lewan and Henry, 2001). GOR derived from the mahogany shale of Green River Formation containing a Type I kerogen (Lewan and Henry, 2001), shows equivalent GOR values to those calculated in this work around 75–90 m^3/m^3 (400–500 scf/bbl) for the oil zone.

A contrary trend for GOR with increasing thermal maturity has been determined through closed system anhydrous pyrolysis at similar experimental conditions. The GOR in these experiments

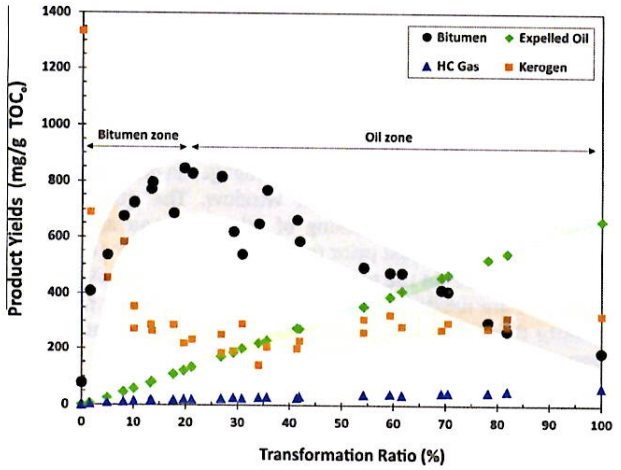

Fig. 3. Product yields generated by hydrous pyrolysis as a function transformation ratio.

systematically increased with thermal maturity (Quigley and Mackenzie, 1988; Lewan and Henry, 2001). These conflicting results have been attributed to the differences in the generated products. Hydrous pyrolysis GOR values are calculated with only the expelled oil and generated gas. Anhydrous pyrolysis generates no expelled oil, so GOR values are calculated with the generated gas and solvent soluble or thermally labile bitumen in the rock. As a result, the anhydrous pyrolysis GOR values increase with temperature as soluble or labile bitumen decreases and generated gas increases to a greater extent than in hydrous pyrolysis (Lewan and Henry, 2001). Moreover, the cross-linking reactions forming pyrobitumen are more prevalent in closed system anhydrous pyrolysis than in hydrous pyrolysis, which result in lower yields of liquid hydrocarbons (Lewan, 1997; Lewan and Roy, 2011).

GOR derived from MSSV pyrolysis and open system pyrolysis-GC also increase as a function of increasing temperature within similar experimental conditions. Non-isothermal pyrolysis temperatures between 340 °C and 360 °C at a heating rate of 0.7 K/min gave GOR values greater than 0.2 kg/kg and significantly increased to values higher than 0.3 kg/kg at TR values above 80% (Duppenbecker and Horsfield, 1990; Santamaría-Orozco and Horsfield, 2003).

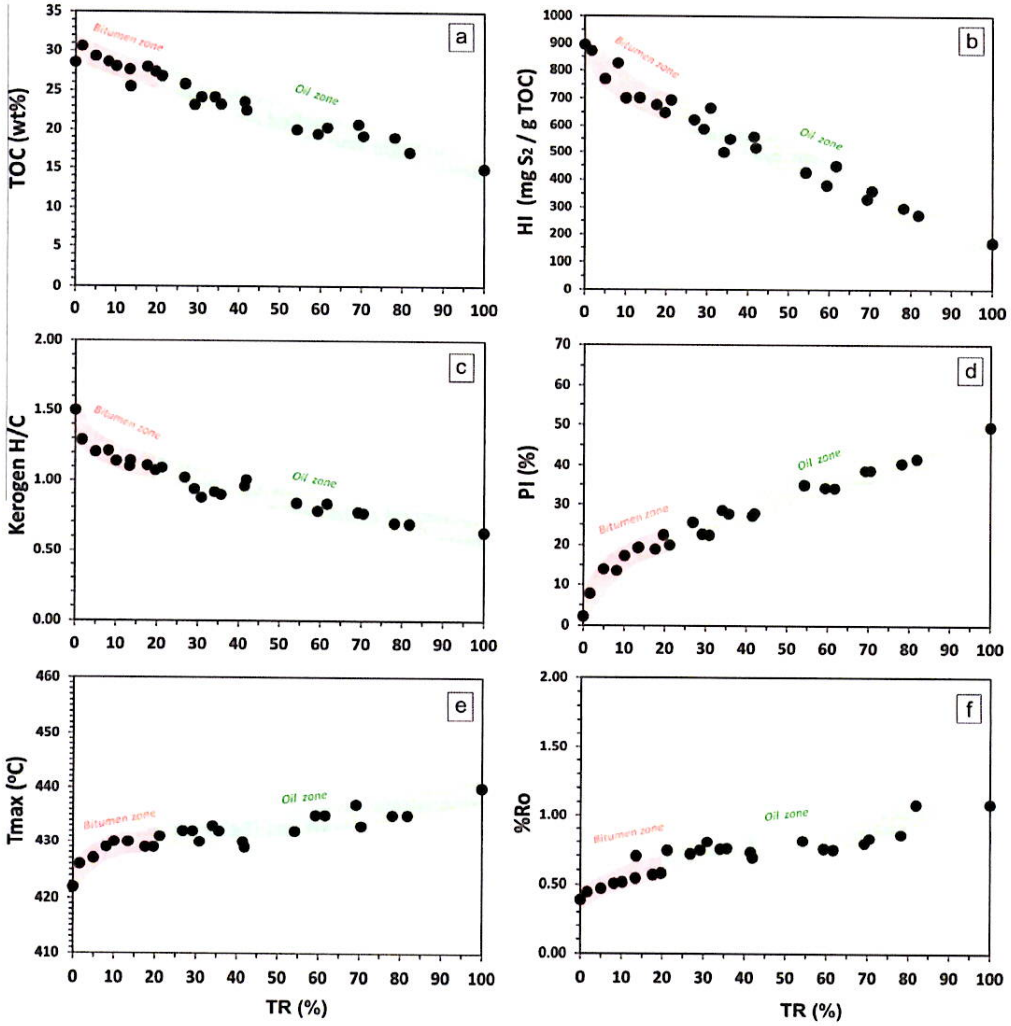

Fig. 4. Thermal maturity indices for a Type I kerogen as a function of transformation ratio (TR). (a) TOC: total organic carbon; (b) HI: hydrogen index; (c) kerogen H/C: hydrogen–carbon atomic ratio; (d) PI: production index; (e) T_{max}: maximum temperature; (f) %R_o: vitrinite reflectance.

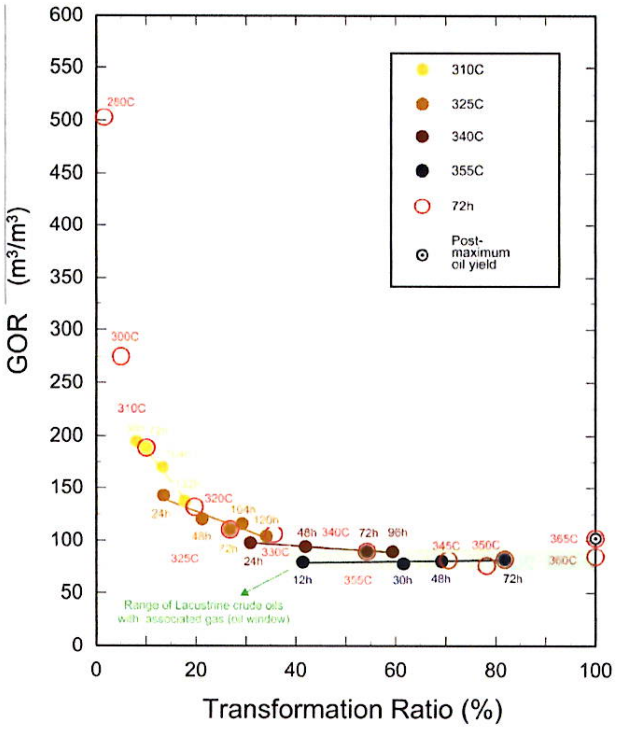

Fig. 5. Evolution of the gas/oil ratio (GOR) with the increase of transformation ratio containing a Type I kerogen based on hydrous pyrolysis experiments and its comparison with natural petroleum.

Expelled oil and gas obtained experimentally in this study compares favorably to the natural data set of lacustrine crude oils with associated gas. Fig. 6 shows a similar relationship between API gravities and GOR values in the oil zone for HP products and natural petroleum occurrences. GORs are characterized by low values between 75–100 m^3/m^3 with no significant variation (Fig. 5), with API gravities ranging from 22–31.9° (Fig. 6). This general agreement supports the use of HP in predicting GOR values during oil generation.

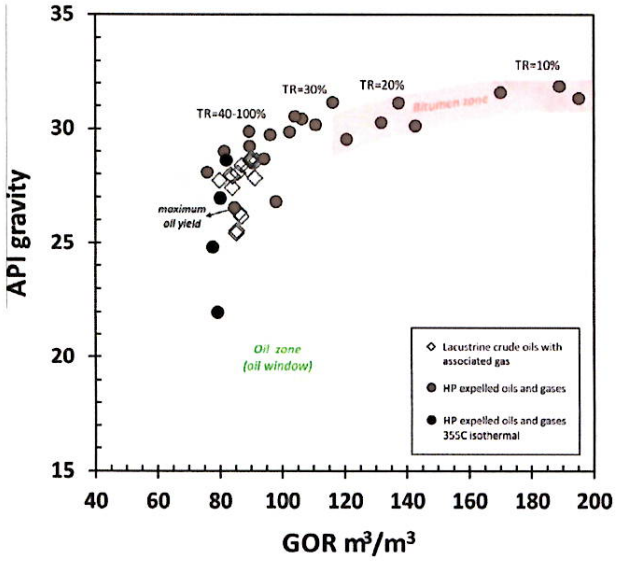

Fig. 6. Gas/oil ratio (GOR) vs API gravity showing the comparison between natural petroleum and hydrous pyrolysis products (HP expelled oil and gas) generated from lacustrine sources (TR = transformation ratio).

With GORs remaining essentially constant through most of the oil window, 1 g of oil may change volume (API gravity) through the thermal decomposition of resins and asphaltenes to non-gaseous saturate and aromatic hydrocarbons and still remain as 1 g of oil. This concept changes the way we view changes in oil compositions during maturation within the oil window. The question that remains is whether this cracking of oil resins and asphaltenes occurs within the rock just prior to oil expulsion or after expulsion while the oil resides in the reactor on the water surface. Additional experiments are needed to address this question, but it raises the possibility that thermal regimes during migration or entrapment influence the oil properties.

3.4. Petroleum fractions

C_{15+} fractions (saturates, aromatics and polars) of bitumens and expelled oils are shown in Fig. 7. This ternary diagram shows that the percentages for the HP expelled oils are similar to natural oils, and there is a definite separation with no overlap between the HP expelled oils and the bitumens as observed in HP of Green River source rocks with Type I kerogen (Ruble et al., 2001). This represents distinct organic phases because the hydrocarbon rich oil is immiscible in the water-bearing bitumen (Lewan, 1997). It is interesting note that the original unheated bitumen has essentially the same amount of polars as the bitumen at a TR of 100%.

Changes in the volatile fraction of the expelled oil and the SARA fractions of the expelled oil and bitumen are given in Fig. 8 on the basis of mg/g TOC_0. The volatile, saturate, aromatic and asphaltene fractions of the expelled oil systematically increases with increasing TR through the bitumen zone and to the end of the oil zone (TR = 100%). The resin fraction of the expelled oil also has a systematic increase with increasing TR, but its increase diminishes slightly above a TR of 60%. Because of the evaporation of the extracting solvent in obtaining bitumen, there is no volatile fraction. The saturate, aromatic, and asphaltene fractions of the bitumen show arcuate trends, with the highest yield occurring at ~50% TR for saturates, ~35% TR for aromatics, and 20% TR for asphaltenes. The resin fraction of the bitumen shows only a systematic decrease through the bitumen zone to the end of the oil zone. Saturates in the bitumen are greater than those in the expelled oil until a TR of ~30%, and are less than those in the expelled oil at higher TR values. Aromatics in the bitumen are also greater than those in the expelled oil, but their dominance continues to a TR value of 35%. Asphaltenes in the bitumen dominate those in the expelled oil over the entire range of TR. Asphaltenes in the bitumen initially increase to a TR value of 20%, which coincides with maximum bitumen generation from the decomposition of kerogen (Fig. 3). These results are in agreement with other studies that report the asphaltenes and resins of the bitumen to be the main source of saturates and aromatic hydrocarbons that are major components in the expelled oil (Ruble et al., 2001; Behar et al., 2008, 2010). Additionally, pyrolysis studies of oil asphaltenes demonstrated that the large structure of the asphaltenes is the source of hydrocarbons (Behar et al., 1984; Cassani and Eglinton, 1986; Mukhopadhyay et al., 1995; di Primio et al., 2000; Spigolon et al., 2010).

3.5. API gravity of oils

The density and API gravity of the expelled oils for each experiment are shown in Table 5. Plots of API gravity of the expelled oils vs. their percentage of volatile and SARA fractions are shown in Fig. 9. There is no relationship between API gravity the volatile fraction (Fig. 9a). API gravity and saturates do show a general

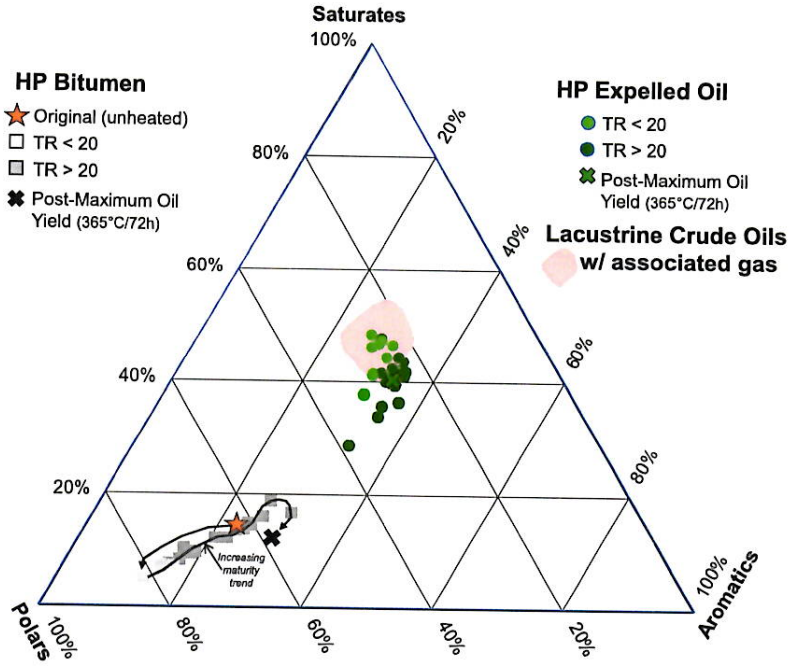

Fig. 7. Comparison of the fractional compositions (C_{15+} saturates, aromatics and polars) of natural crude oils and hydrous pyrolysis products (HP bitumens and expelled oils) from lacustrine sources during the oil window.

positive relationship (Fig. 9b). Aromatics do not have a decisive relationship with API gravity (Fig. 9c), but the resin and asphaltene fractions (as polars) do have a negative relationship (Fig. 9d–f). Asphaltenes have the best linear relationship and are the most influential in determining API gravity of the oils.

The ranges of asphaltenes and API gravity obtained experimentally are comparable to those measured in lacustrine natural black oils (Fig. 10). This similarity suggests that the mechanism of generation, decomposition and expulsion of asphaltenes under HP conditions represents what occurs in the natural system. In general, the increase of API gravity is directly related to the decrease of asphaltene content or the increase of saturates of the oils following the maturation trend. For the black oils generated during the oil window, it is possible to distinguish two main domains: heavier oils (22–27° API) with the asphaltene content ranging from 10–17%, and lighter oils (28–30° API) ranging from 4–9%. Asphaltene contents of < 2% are associated with light oils and condensates with API gravity higher than 35° (Fig. 10). Similar ranges were also reported by Khavari-Khorasani et al. (1998) in oils from the Gulf of Suez.

The relationship of API gravity with TR is more complex than typically envisioned as shown in Fig. 11 (Spigolon et al., 2013). The expelled oils from the temperature series for 72 h shows a gradual decrease in API gravity from 31.9° at 310 °C/72 h to 26.5° at 360 °C/72 h (Table 5). This decrease suggests that more asphaltenes and less saturates are being expelled with the oil as TR increases. For the time series experiments this moderate API gravity decrease with TR becomes more complex (Fig. 11). API gravities for oils from the 310 °C time series are the highest (31.1–31.9°), and plot on the temperature 72 h series trend with no systematic change with time (Fig. 11). This indicates that the amounts of asphaltenes and saturates expelled in the oils within the bitumen zone (TR < 20%) are essentially in the same proportions. The small amounts of oils expelled in this early stage of maturation may be due to the preferential expulsion of these compounds relative to the retention of heavier compounds in the source rock (Sandvik et al., 1992). The 325 °C time series shows a slight increase in API gravity with increasing time and TR, but the range is narrow (29.5–31.2°) and it straddles the temperature 72 h series trend, as well as maximum bitumen generation. The increase in API gravity with increasing time becomes more pronounced in the 340 °C and 355 °C time series experiments (Fig. 11). API gravities for the 340 °C time series systematically increase with time from 26.8° at 24 h (TR = 30.9%) to 29.9° at 96 h (TR = 59.4%). API gravities for the 355 °C time series also systematically increase with time, but over a greater range from 22.0° at 12 h (TR = 41.4%) to 28.6° at 72 h (TR = 81.8%). This more pronounced changes in API gravity may be explained in part by less saturates and more asphaltenes being expelled with increasing time after maximum bitumen generation (TR = 20%) and decomposition of bitumen to hydrocarbon rich oil commences at the higher temperatures. However, the data indicate that other factors may also be responsible. In particular, oil generated at 355 °C after 12 h has an API of 22° at a TR of 41.4%, and at essentially the same TR (i.e., 41.9%), the oil generated at 340 °C after 48 h has an API of 28.6°. These results indicate that temperature and TR alone are not responsible for API gravity and that time also plays an important role in determining the amounts of saturates and asphaltenes expelled with an oil. Although more experimental work is needed to fully understand this relationship, one tentative explanation is that the oils may thermally mature in the reactor as they accumulate on the water surface. Their thermal maturation in this context entails the thermal decomposition of the asphaltenes and possibly the resins in the expelled oils to saturates and aromatics. Because the GOR values are unchanged within this range of TR values (Fig. 5), no significant gas generation is associated with this secondary thermal maturation. At a given TR, the mass of oil expelled from a source rock is the same at varying temperature and time conditions, but its volume (API gravity) may vary with varying temperature and time conditions. One implication here is that the thermal history during the migration and accumulation of an expelled oil may determine in part its SARA

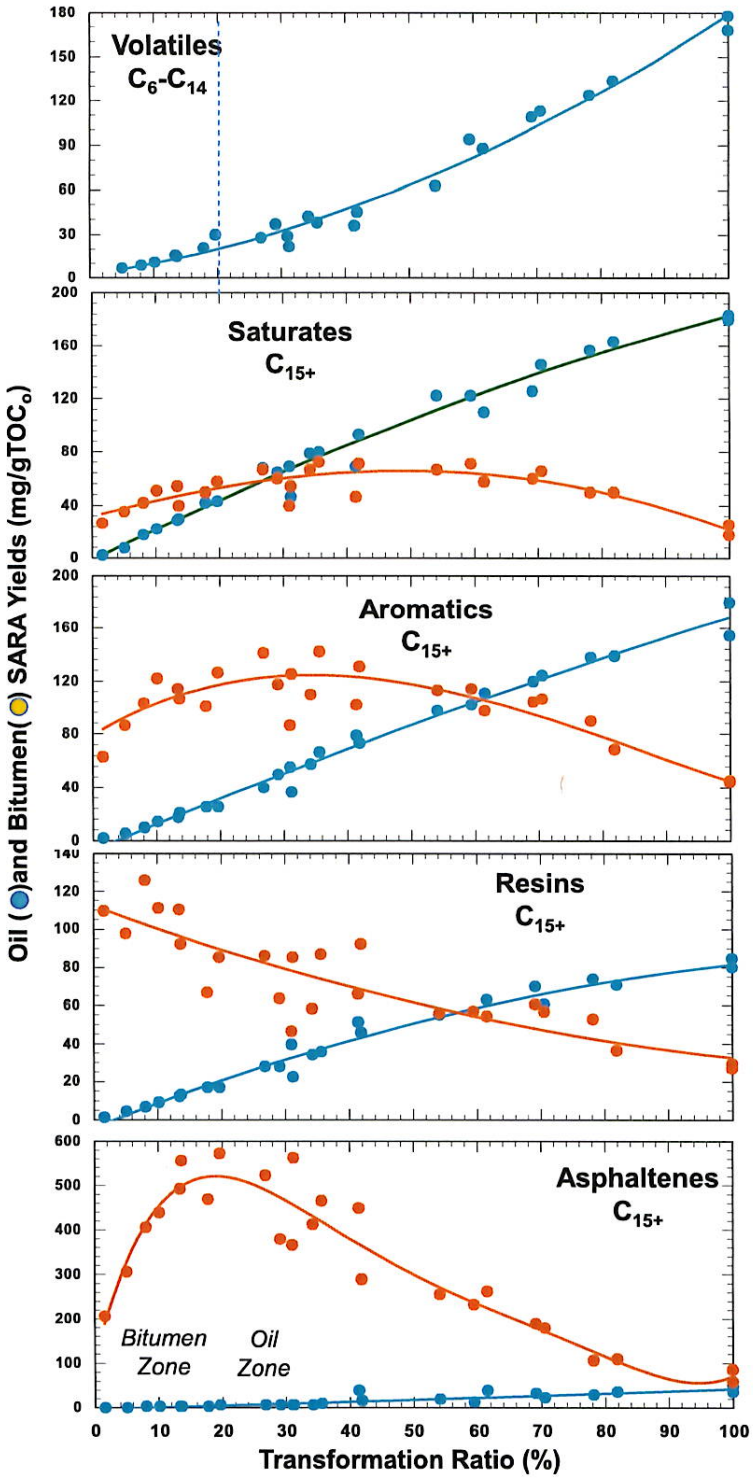

Fig. 8. Comparison of changes in the expelled-oil volatiles (C_6–C_{14}) and C_{15+} SARA fractions of expelled oil and bitumen with transformation ratio. Curves are polynomials used to show general trends.

composition and API gravity. Future field and experimental studies are needed to determine whether this complexity is unique to Brazilian Type I kerogen, an artifact of HP conditions, or a new insight on natural controls on oil API gravity.

Changes in API gravity have been observed by many authors in the natural system as a consequence of increasing thermal maturation associated with burial depth. However, the original fluids produced can be affected by complex phenomena such as

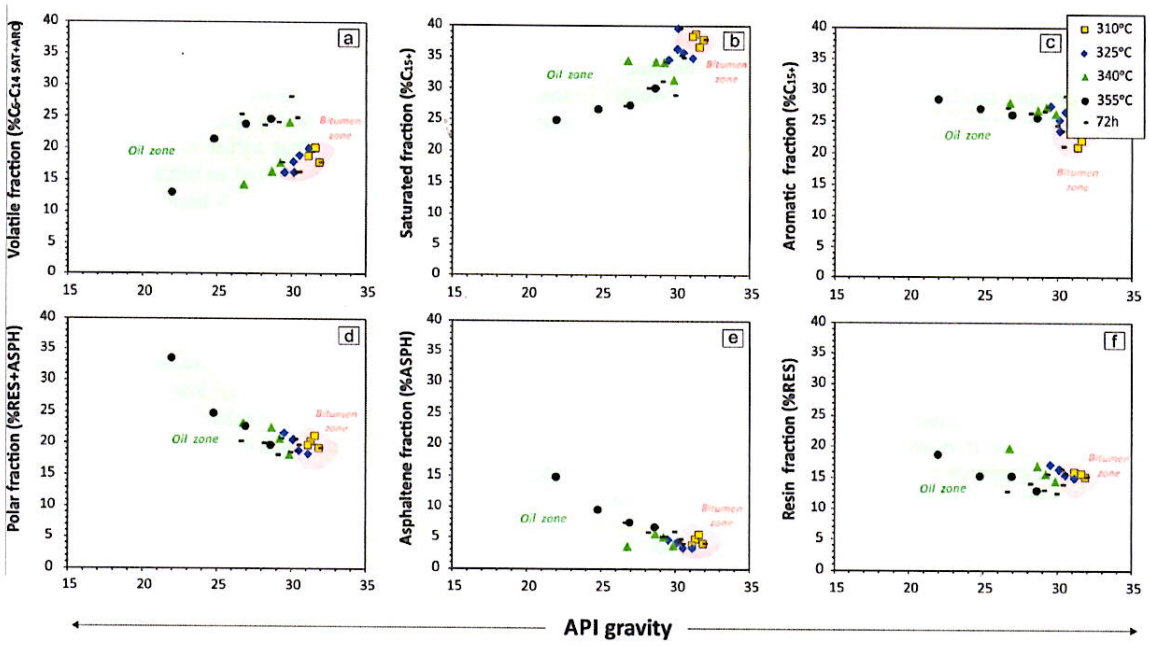

Fig. 9. Relationship between API gravity and fractional compositions of the expelled oils generated by hydrous pyrolysis for a Type I kerogen. (a) Polar fraction; (b) asphaltene fraction; (c) resin fraction; (d) volatile fraction; (e) saturated fraction; (f) aromatic fraction.

expulsion, migration and a variety of alteration processes, which also promotes changes in the composition, especially in terms of bulk properties. In most cases, there is not a direct relationship between API gravity and depth or temperature (Tissot and Welte, 1984; Blanc and Connan, 1993; Hunt, 1996; Radke et al., 1997; Guthrie et al., 2012). It is important to emphasize that the migration effect is minimized due to the short distance of migration (centimeters) experienced in hydrous pyrolysis compared to natural secondary migration through carrier beds for tens to hundreds of kilometers. In addition, variations in solubility of saturates with aromatics and resins (Orr, 1986), or the solubility of water in the bitumen network of a source rock (Lewan, 1997) may be critical factors in determining API gravity of expelled oil. Adsorption and retention phenomena of different petroleum fractions as proposed by Rudkiewicz and Behar (1994) may also play an important role in determining the API gravity of expelled oils. Moreover, the oil retention capability may be reduced with the development of fractures and voids in a source rock during the oil generation (Souza et al., 2014). This would also facilitate the expulsion of asphaltenes

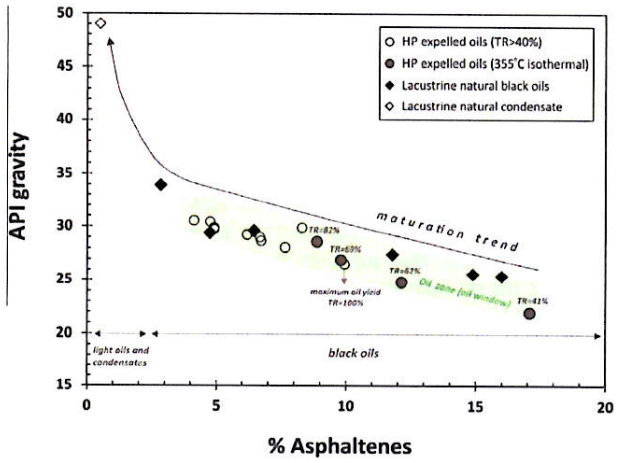

Fig. 10. Relationship between asphaltene content and API gravity of hydrous pyrolysis and natural oils generated from lacustrine source rocks with Type I kerogen from Lower Cretaceous.

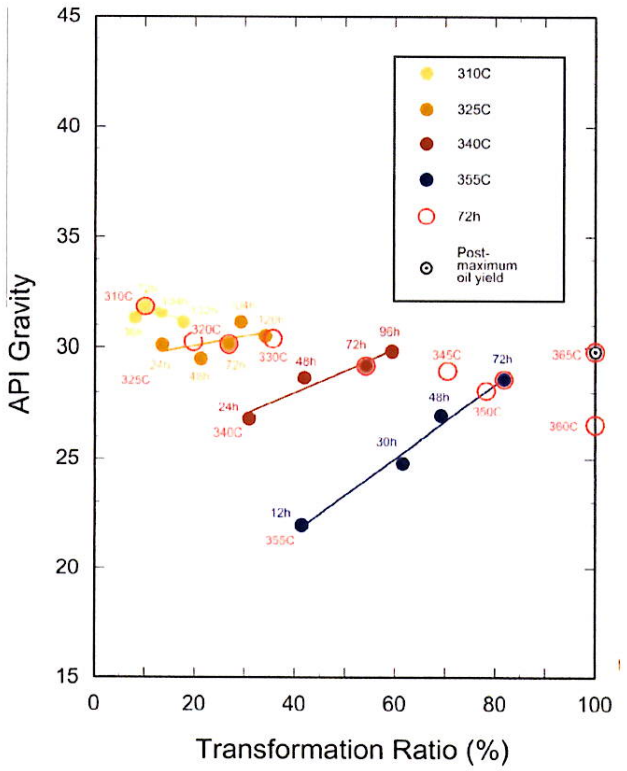

Fig. 11. API gravities of expelled oils generated by hydrous pyrolysis as a function of the transformation ratio (TR) for a Type I kerogen.

from a source rock, which would result in a decrease in the API gravity of the expelled oil. Although the complexity of predicting oil quality (e.g., API gravity and GOR) may be daunting, HP provides a laboratory method that can be used in conjunction with natural data to help resolve the complexity and test hypotheses.

3.6. Sulfur content

The sulfur contents of the expelled oils obtained for each experiment are presented in Table 5. As a general trend, sulfur contents decrease systematically with increasing transformation ratios in both temperature and time series experiments. The sulfur contents are higher (around 1.5–1.2%) in early generated oils at lower maturity levels corresponding to the bitumen generation stage (TR < 20%), whereas late generated oils at TR values greater than 40% during the oil generation stage tend to have lower sulfur contents around 0.8–1.0%. It is worth noting that for any given value of TR, the sulfur contents are higher for those oils generated and expelled under lower isothermal conditions, an observation that also suggests a time–temperature dependency.

Fig. 12 shows the relationship between sulfur contents and API gravities of expelled oils generated by hydrous pyrolysis. These oils are characterized as medium sulfur contents according to the scheme proposed by Orr (2001) for Type II and IIS kerogens from the Monterey Formation. Most expelled oils follow a negative linear trend, which is controlled by maturity, as observed by Orr (2001). This is evident in the expelled oils generated at isothermal temperatures of 325 °C, 340 °C and 355 °C, which show linear trends of decreasing sulfur content as API gravity increases with increasing TR values. The oils expelled early at TR < 20% are the exception, with higher sulfur contents and API gravity, but with no large compositional variations during the bitumen generation stage (Fig. 12). As previously suggested, these oils may be result of preferential expulsion of lighter compounds (mostly saturated and aromatics) relative to polars.

Compared with the natural system, the lacustrine crude oils of the Lower Cretaceous contain lower contents of sulfur (Fig. 12). This difference can be attributed to facies variations in the source rock with different sulfur contents. Another possibility would be that HP expelled oils exaggerated sulfur contents as result of shorter distances (cm) of migration compared with natural secondary migration through carrier beds for tens to hundreds of kilometers.

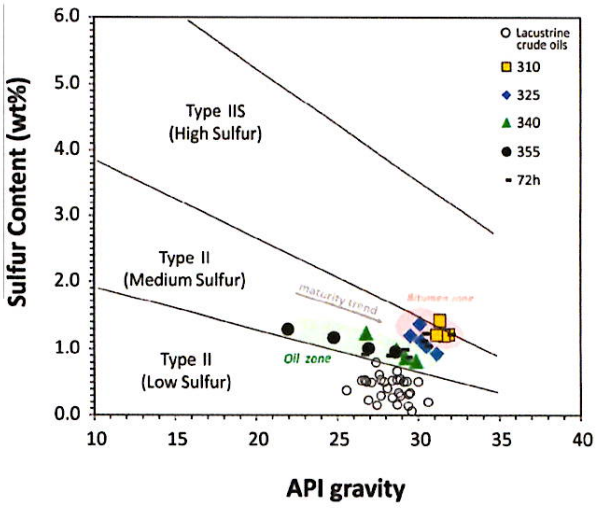

Fig. 12. Relationship between sulfur content and API gravity of expelled oils generated by hydrous pyrolysis and their comparison with natural oils (based on Orr, 2001).

In summary, relatively high percentages of sulfur obtained in the expelled oils are genetically associated with intermediate organic sulfur content in the kerogen used in this work, which is about 2.8%. This suggests that sulfur compounds in the original kerogen can be rapidly transferred to bitumen and oil due to the lower energy required to break C–S bonds. As a consequence of weak sulfur linkages, oils expelled early during the initial stage of thermal maturation are associated with higher sulfur contents, which gradually decrease as a result of the dilution effect related to the significant increase of the expelled oil yields during oil generation. According to Lewan (1985) and Baskin and Peters (1992), kerogen that commonly contains abundant chemically bound sulfur is responsible for early, low temperature generation of bitumen and heavy oils rich in sulfur. This is observed in the first oils expelled at TR values > 40% in the time series experiments at 340 °C and 355 °C (Table 5 and Fig. 12).

3.7. GC-amenable composition

Systematic changes with increasing transformation ratio were observed in the overall compound distribution measured by GC-FID of bitumens and expelled oils generated by hydrous pyrolysis (Table 6). It is important to emphasize that < 40 wt% of oil is characterized by GC (Martin et al., 1963). Molecular ratios used in this work were based on the integration of GC peak areas. Significant changes in the proportions of normal and branched alkanes in HP bitumens and expelled oils were observed with increasing thermal maturity, as also observed in the natural system. Fig. 13 shows a reasonable correlation between the whole oil gas chromatograms and geochemical properties of HP expelled oils and lacustrine crude oils generated from Brazilian source rocks of Lower Cretaceous containing Type I kerogen. For each experiment, it is quite evident that the proportions of normal alkanes in the GC traces of expelled oils increase relative to the isoprenoids with increasing transformation ratio (Fig. 13a). This behavior is also apparent in the pristane/n-C_{17} and phytane/n-C_{18} ratios of bitumens and expelled oils, which show a systematic decrease with increasing transformation ratio (Fig. 14a and b). Positive correlations were obtained with Brazilian lacustrine crude oils from Lower Cretaceous source rocks (Fig. 13a and b). Although these ratios are good maturity indices for oils within the oil window, there are variations in these trends for different lacustrine source rocks containing Type I kerogen of Tertiary age (Ruble et al., 2001; Binotto et al., 2010). This indicates that original organic matter input and depositional conditions have control on these ratio trends and limits their use as standalone maturity indices.

Pristane/phytane ratio in expelled oils is constant but slightly higher than those in the corresponding bitumens (Fig. 14c). The decrease of this ratio in bitumens was also reported by other authors in natural series related to Type II kerogen (Tissot et al., 1971; Sagjo, 1980). This suggests that pristane is preferentially expelled in the oil relative to phytane. Carbon preferential indices of bitumens and expelled oils (CPI) are different at low TR values (< 10%), but converge at higher TR values (Fig. 14d).

It is also clear that the fraction of normal alkanes to whole oils (given by their relative areas in the GC trace) in expelled oils vary according to the time–temperature conditions of the hydrous pyrolysis experiments (different values for the same TR; Table 6). Based on the results of quantitative GC analyses, one can estimate that only 3.9–12.1% of the oils are composed of n-alkanes (%n-C_6–C_{35} in Table 6).

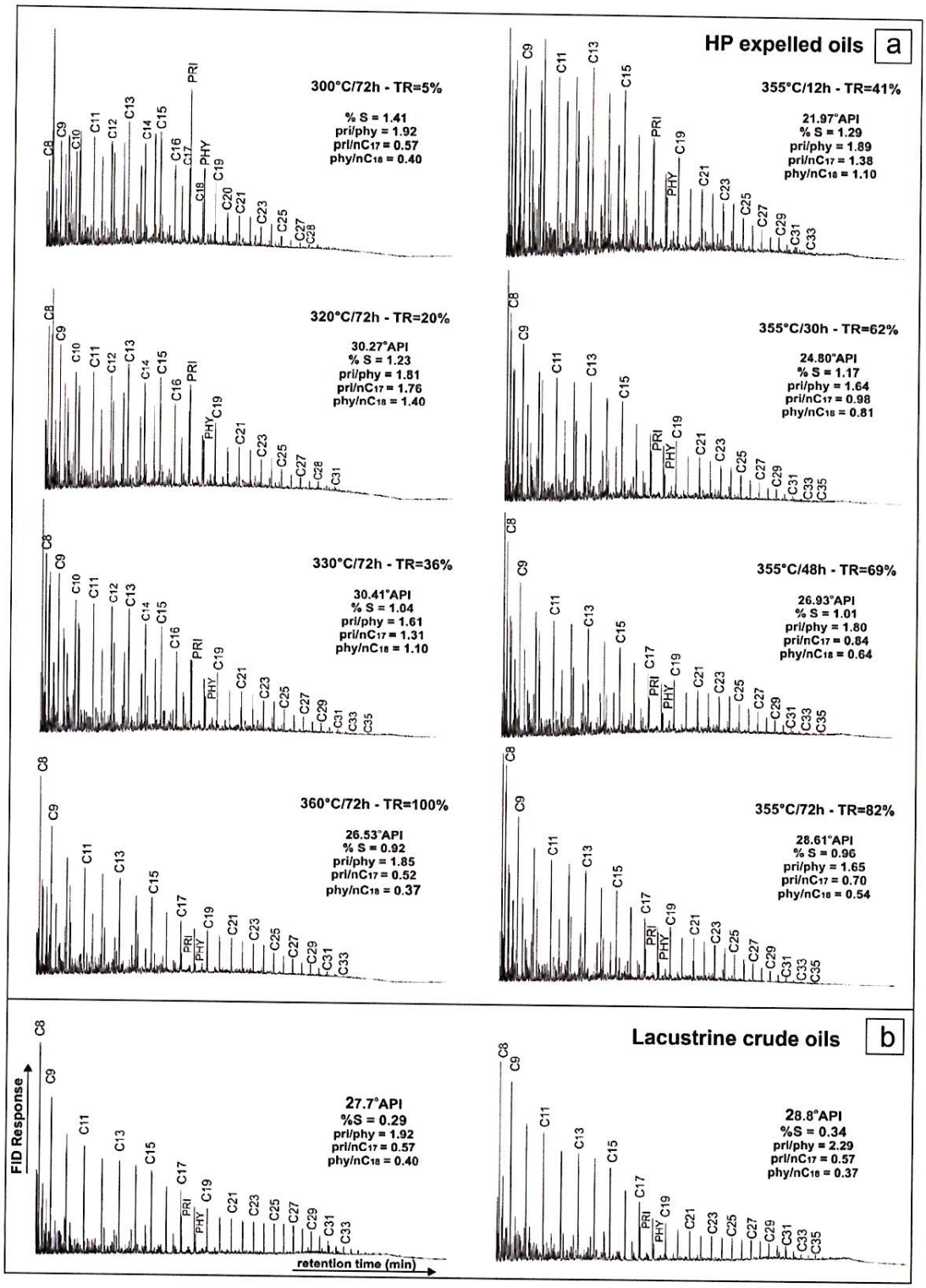

Fig. 13. Gas chromatograms and geochemical properties of expelled oils generated by hydrous pyrolysis with their associated transformation ratio (a) compared to lacustrine crude oils (b).

3.8. Generated gas composition

Yields and molecular indices of gases generated by hydrous pyrolysis as a function of transformation ratio (TR) are given in Table 7 for temperature series experiments and in Table 8 for time series experiments. The amount of each hydrocarbon gas (C_1–C_5) increases with increasing transformation ratio. Methane (CH_4) is the major hydrocarbon compound followed by ethane (C_2H_6), propane (C_3H_8), butane (iso+n-C_4H_{10}) and propane (iso+n-C_5H_{12}). Among the non-hydrocarbon gases, carbon dioxide (CO_2) is the

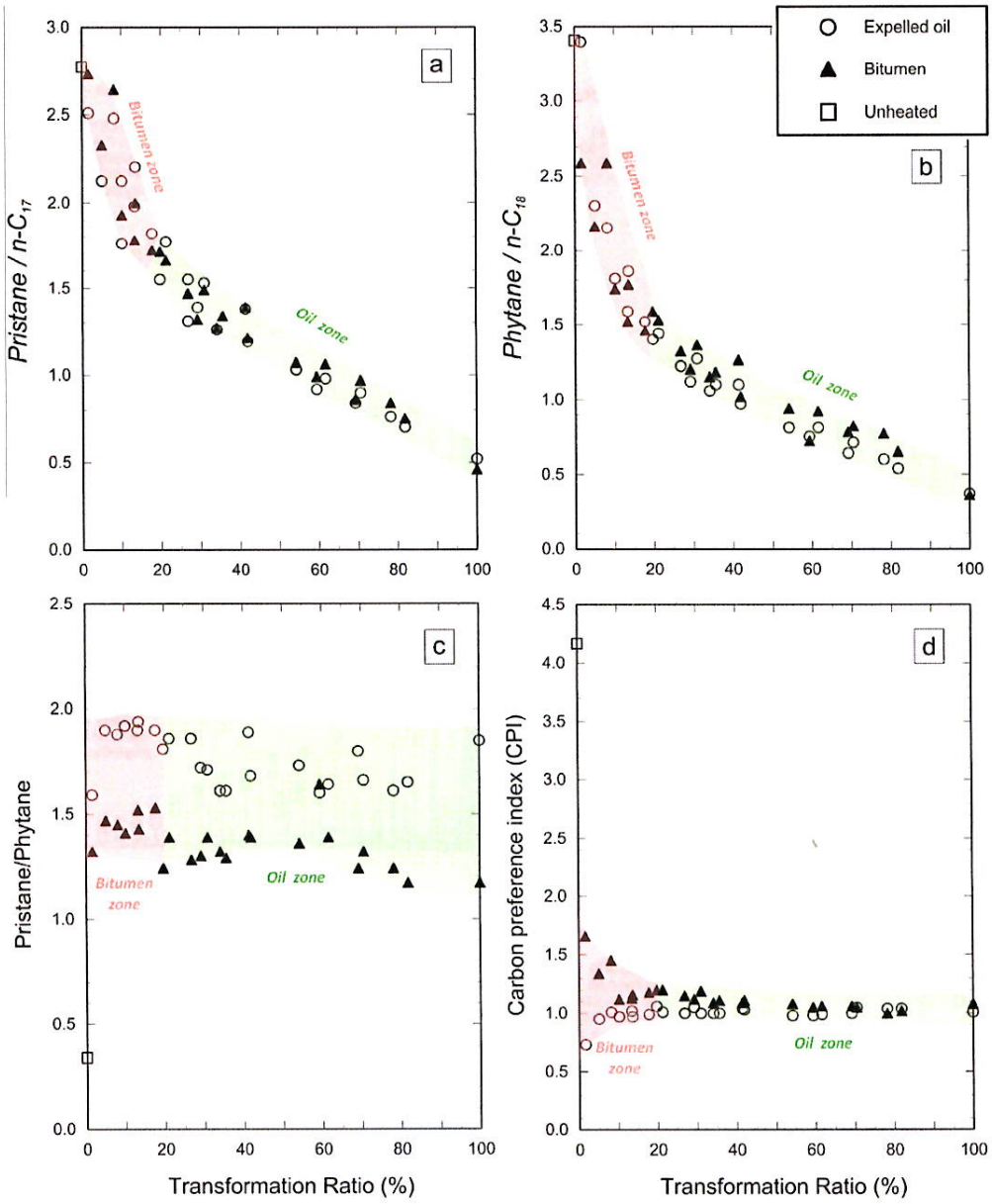

Fig. 14. Molecular ratios based on peak areas measured on the GC traces of bitumens and expelled oils generated by hydrous pyrolysis with increasing transformation ratio. (a) pristane/n-C_{17}; (b) phytane/n-C_{18}; (c) pristane/phytane; (d) carbon preference index – CPI.

most abundant followed by molecular hydrogen (H_2) and nitrogen (N_2). No hydrogen sulfide (H_2S) was detected. Due to their high solubility, a significant portion of generated H_2S and CO_2 is dissolved in the water (Lewan, 1997). The lack of high CO_2 contents in natural gases can be explained by its high solubility in water and its reactivity with calcium in the water of carrier beds to form carbonate cements. Moreover, H_2S can react with Fe based stainless steel surfaces to form pyrrhotite ($Fe_{1-x}S$; Lewan, 1993a). This reaction with reactor walls composed of stainless steel 316 is minimal and more so with the Ni based Hastelloy C276 (Lewan, 1993a), which was used in this study. However, the gas collection cylinders are composed of less resistance stainless steel 304, which is assumed to have reacted with the H_2S in the collected gas to form pyrrhotite. As a result, the analyses of the collected gases yielded no detectable H_2S. Future studies should use collection cylinders coated with a nonreactive material (e.g. Sulfinert®) to avoid this problem. It should also be noted that the collected gases in this study resided in their cylinders for more than 4 weeks before being analyzed.

Molecular indices were used to evaluate the proportionality among gases generated with increasing thermal maturation during the bitumen and oil zones (Fig. 15).

The carbon dioxide index [$CO_2/(CO_2 + CH_4)$] decreases systematically with increasing transformation ratio, suggesting that most of CO_2 was generated in the early stages of thermal maturation (Tables 7 and 8; Fig. 15a). According to Seewald et al. (1998), large amounts of CO_2 are produced from decomposition of kerogen and bitumen in the presence of water.

The behavior of gas dryness expressed by the ratio between methane and heavier HC gases (i.e., C_2–C_5) was monitored through

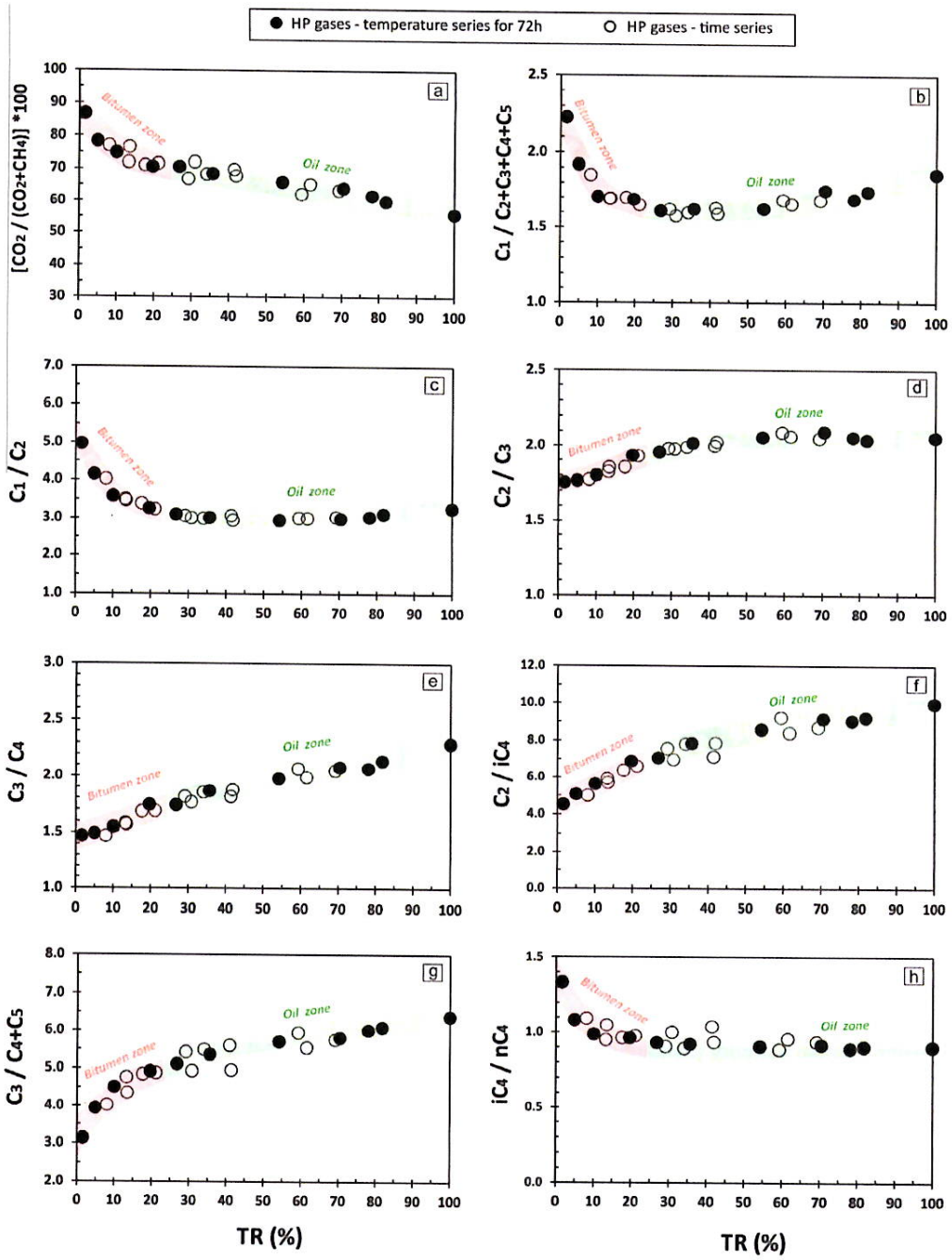

Fig. 15. Molecular indices of gases generated by hydrous pyrolysis and their evolutionary trends with the increase of transformation ratio (TR) during the bitumen and oil zones. (a) $[CO_2/(CO_2 + CH_4)] * 100$; (b) $C_1/C_2 + C_3 + C_4 + C_5$; (c) C_1/C_2; (d) C_2/C_3; (e) C_3/C_4; (f) C_2/iC_4; (g) $C_3/C_4 + C_5$; (h) iC_4/nC_4.

the indices $C_1/(C_2 + C_3 + C_4 + C_5)$, $C_1/(C_2 + C_3)$ and C_1/C_2 (Tables 7 and 8 and Fig. 15b and c). During the bitumen zone (TR < 20%), the highest values of these indices indicate that methane is the predominant gas. The dryness of the gas decreased with increasing TR to about 20% and then remains relatively constant through the oil zone. A slight increase in gas dryness can be observed starting near the maximum oil yield at TR > 70%.

According to Hunt (1996), the initial thermogenic gas generated from kerogen is relatively dry at a low thermal maturity (< 0.5 $\%R_o$). Seewald et al. (1998) also observed through hydrous pyrolysis experiments that low maturity gas produced via primary cracking of kerogen is composed predominantly of methane.

On the other hand, HP gases generated during the oil zone at TR > 20% are especially enriched in the wet fraction (C_{2+}), as observed in natural gases generated during the oil window depending on kerogen type (Evans et al., 1971). Wet gas indices such as C_2/C_3 (Fig. 15d), C_3/C_4 (Fig. 15e), C_2/i-C_4 (Fig. 15f) and $C_3/(C_4 + C_5)$ (Fig. 15g) presented similar and systematic increases with increasing transformation ratio, but smaller ranges were noted for C_2/C_3. Conversely, i-C_4/n-C_4 index decreases to a TR value of 20% and then remains relatively constant at higher TR values (Fig. 13h).

All ranges of the molecular indices ($C_1/(C_2 + C_3)$, C_2/C_3, C_2/i-C_4, C_3/C_4, i-C_4/n-C_4) obtained in this work are equivalent to primary thermogenic gases generated by primary cracking of kerogen and

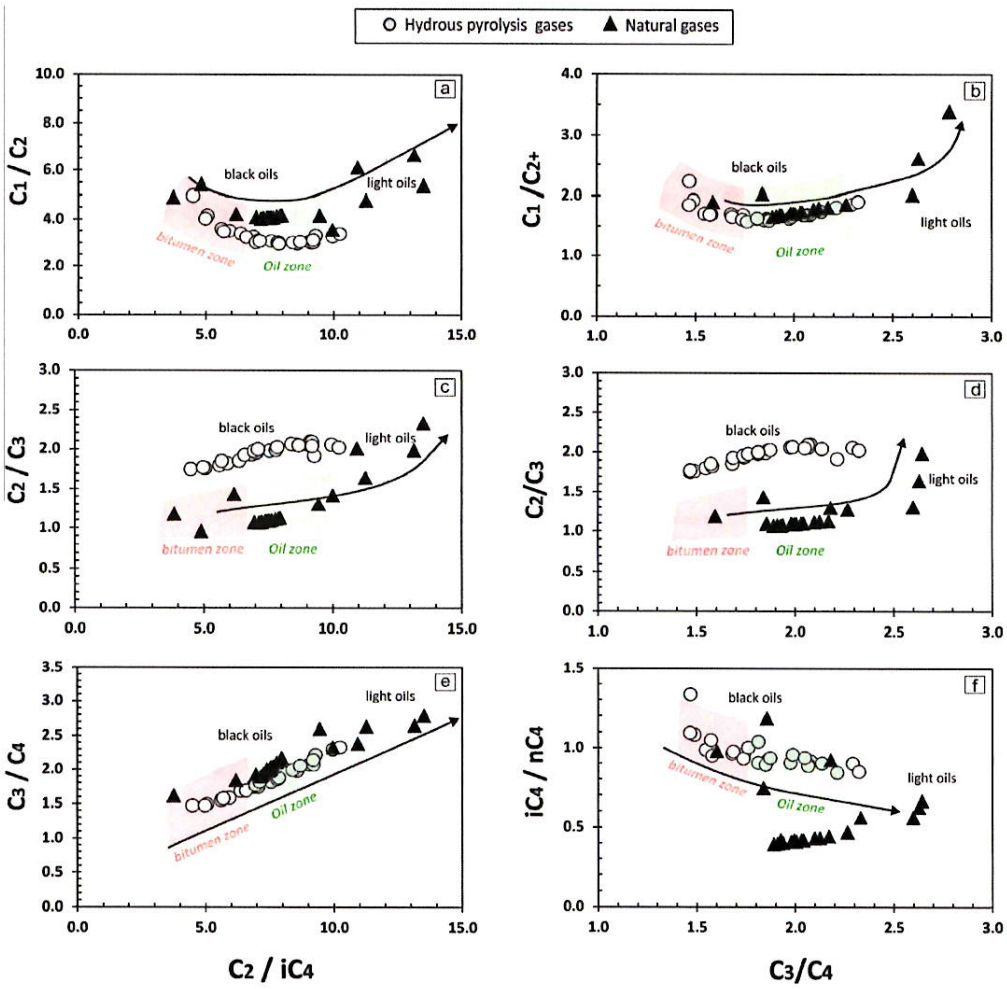

Fig. 16. Comparison of molecular indices of natural and hydrous pyrolysis gases generated from lacustrine source rocks of the Lower Cretaceous containing Type I kerogen. The black arrow indicates the evolutionary pathway of the maturity trend. (a) C_1/C_2 vs C_2/iC_4; (b) C_1/C_{2+} vs C_3/C_4; (c) C_2/C_3 vs C_2/iC_4; (d) C_2/C_3 vs C_3/C_4; (e) C_3/C_4 vs C_2/iC_4; (f) iC_4/nC_4 vs C_3/C_4.

bitumen with increasing thermal maturity (Bernard et al., 1978; Schoell, 1983; Oudin, 1993; Prinzhofer and Huc, 1995; Lorrant et al., 1998; Prinzhofer et al., 2000).

Fig. 16 shows a direct comparison with molecular indices of natural gases generated from Brazilian lacustrine source rocks of the Lower Cretaceous with Type I kerogen. The HP gases showed that the proportion of methane (dry fraction) and the wet fraction are very similar to those produced in the natural system during the oil window, resulting in a very close C_1/C_{2+} index (Fig. 16b). However, the greatest differences are in the wet fraction with high proportions of ethane (C_2) in the HP gases. The excess of ethane generated by hydrous pyrolysis is most evident in its effect on the C_1/C_2 and C_2/C_3 ratios, which do not compare with the natural gases (Fig. 16a, c and d). This enhanced ethane has also been observed in other pyrolysis studies (di Primio and Horsfield, 2006; Kotarba and Lewan, 2013). Despite this deviation, gases generated artificially by hydrous pyrolysis compared well with natural primary gases associated with oil (Kotarba et al., 2009; Kotarba and Lewan, 2013).

The indices C_3/C_4 vs C_2/i-C_4 showed a good correlation between natural and HP gases generated for lacustrine sources (Fig. 16e). However, some discrepancies were observed for the i-C_4/n-C_4 index, which shows a great variability in the oil zone ranging from 0.4–1 (Fig. 16f). Generally, this index tends to decrease with the increasing thermal maturation according to Oudin (1993), who prescribe values < 1 for thermogenic gases generated during oil window.

4. Conclusions

The Green River Formation has been considered the classic example of Type I kerogen. However, Brazilian source rocks with Type I kerogen have been the source of vastly greater quantities of petroleum. In this study, we evaluate the composition and quality of petroleum generated prior to secondary gas generation (i.e., oil window) from a Brazilian source rock with Type I kerogen using hydrous pyrolysis. Results show that similar to other oil prone source rocks, kerogen initially decomposes in part to a polar rich bitumen, which decomposes in part to hydrocarbon rich oil with increasing thermal maturation. These two overall reactions overlap with one another and have been recognized in oil shale retorting and natural petroleum generation. During bitumen decomposition to oil, some of the bitumen is converted to pyrobitumen, which results in an increase in the apparent kerogen (i.e., insoluble carbon) content with increasing maturation.

Expelled oil generated from the source rock by hydrous pyrolysis provides a means of calculating an oil generation

transformation ratio (TR) that can be used to collectively evaluate temperature- and time-series experimental results within the oil window (TR = 0.0–100%). Rock–Eval data on the recovered rock showed similar trends observed in natural maturation with hydrogen indices decreasing from 900–150 mg/g TOC, T_{max} increasing from 422–440 °C, and production indices (PI) increasing from 0–52%. As expected, the atomic H/C ratio of kerogen isolated from the recovered rock decreased from 1.50–0.63.

Generated gas and expelled oil from hydrous pyrolysis within the oil window provide gas/oil ratios (GOR) and oil API gravities that are comparable to those in the natural system. Unlike previously proposed models for increasing GOR in the oil window based on anhydrous pyrolysis, the GOR values from hydrous pyrolysis initially decreased from 508–90 m^3/m^3 at a TR of ~50% and then remain essentially constant to a TR of 100%. The relationship between these GORs and the API gravities of the HP oils are in good agreement with natural relationship between GORs and API gravities of natural crude oils considered to be sourced from Brazilian lacustrine source rocks with Type I kerogen of Lower Cretaceous.

The API gravities of expelled oils from hydrous pyrolysis are in the same range of values as natural crude oils. Asphaltene content has the biggest influence on oil API gravities, and aromatic content has the least influence on oil API gravities. Natural crude oils and expelled oils from hydrous pyrolysis follow the same relationship between percent of asphaltenes and API gravity. The HP experiments show that the relationship between API gravity and thermal maturation within the oil window is more complex than previously thought. Temperature series HP experiments show API gravities of the expelled oils decreasing from 32–27° with increasing maturation within the oil window. However, time series HP experiments show API gravities of expelled oils to increase with time for TRs values > 20% from 22–31°. These changes in API gravity with thermal maturation are interpreted as a result mainly of polars (asphaltenes and resins) in the oil thermally cracking to non-gaseous hydrocarbons (saturates and aromatics) at higher temperatures and longer times. This is not thermal cracking of the hydrocarbons in the oil to secondary gas, but rather the cracking of polars in the oil to saturate and aromatic hydrocarbons. It remains to be determined whether this cracking of oil polars to hydrocarbons occurs in the rock prior to expulsion or after expulsion when the oil is accumulating on the water surface during the experiments. If the latter is the situation, the HP experiments indicate that the thermal history of expelled oils during their migration and accumulation may influence their API gravities. Additional experimental work is needed to resolve this implication.

Sulfur content of the expelled oils is related to asphaltene and resin content, and a negative correlation, as exists in sulfur-API gravity relationship for natural crude oils. However, compared with natural crude oils considered to be sourced from similar Type I kerogen, the HP expelled oils have higher sulfur contents. This is attributed to a possible difference in the organic facies of the natural oils or an exaggeration of sulfur partitioning between the source rock and expelled oils by HP.

GC traces of the expelled oils show *n*-alkane and isoprenoid distributions similar to natural crude oils. With increasing TR values through the oil window (TR > 20%), expelled oils show the full range of *n*-alkanes (C_8–C_{35}), pristane/phytane ratio fluctuations between 1.6 and 1.9, CPI fluctuations between 0.98 to 1.04, and decreasing pristane/*n*-C_{17} and phytane/*n*-C_{18} ratios from 1.8 and 1.5 to 0.5 and 0.4, respectively. With the exception of the pristane/phytane ratio, these GC parameters are essentially the same for the corresponding bitumens. Pristane/phytane ratio of the bitumen (1.2–1.5) is consistently lower than that of the expelled oil, which should be considered in oil-source rock correlations.

Generated hydrocarbon gases are initially dry with a $C_1/\Sigma C_2$–C_5 index of 2.2. This decreases during bitumen generation to a TR of 20% and then increases to 1.9 at a TR of 100%. C_3/C_4 vs $C_1/\Sigma C_2$ and C_2/i-C_4 ratios show a similar curvilinear relationship of the HP gases and the natural gases associated with the natural crude oils considered to be from Type I kerogen. Plots of C_3/C_4 ratios vs C_2/C_3 and i-C_4/n-C_4 ratios do not show similar trends between the HP gases and natural gases. More research on pyrolysis gases is needed within their stable carbon isotopes.

The general overall agreement in composition of natural petroleum supports the utility of hydrous pyrolysis to better characterize petroleum systems and the effects of maturation on petroleum quality within petroleum systems. HP provides a distinct advantage over dry pyrolysis methods by its ability to generate a pyrolysate that is compositionally similar to natural petroleum and expels it in a manner that is operative in the subsurface of sedimentary basins. Like with all pyrolysis methods, new insights gained from hydrous pyrolysis must be evaluated as being previously unrecognized phenomenon in the natural process of petroleum formation or artifacts of the higher temperatures and shorter times used in the experiments.

Acknowledgments

This research was undertaken as part of the first author's Ph.D. and financially supported by Petrobras. This work was in collaboration with ongoing research on petroleum quality at the U.S. Geological Survey (USGS) and with Federal University of Rio de Janeiro (UFRJ).The authors are grateful to the Geochemistry Lab personnel of Petrobras Research and Development Center (CENPES), USGS Energy Resources Program Lab (Denver), with special thanks to Augusta Warden, Zachary Lowry and Mark F. Dreier for analytical support. Support from the Organic Facies and Palynofacies Labs (LAFO/UFRJ), particularly Joalice de Oliveira Mendonça is greatly appreciated. We thank the assistance given by Mário Assine (UNESP), Mitsuru Arai (Petrobras/CENPES), Diógenes Custódio de Oliveira (Petrobras/UO-RNCE) and Idalécio Freitas (Geopark Araripe) in the collection of the outcrop sample used in this study. The authors also appreciated the helpful contribution of the reviewers Daniel M. Jarvie and an anonymous reviewer.

Associate Editor—**Andrew Murray**

References

Abbassi, S., George, S.C., Edwards, D.S., di Primio, R., Horsfield, B., Volk, H., 2014. Generation characteristics of Mesozoic syn- and post-rift source rocks, Bonaparte Basin, Australia: new insights from compositional kinetic modelling. Marine and Petroleum Geology 50, 148–165.

Allred, V.D., 1966. Kinetics of oil shale pyrolysis. Chemical Engineering Progress 62, 55–60.

Agency of Petroleum, Natural Gas and Biofuels (ANP), 2014. Oil, Natural gas and Biofuels Statistical Yearbook, 71 pp.

Assine, M.L., 2007. Bacia do Araripe. Boletim de Geociências da Petrobras 15, 371–387.

Baskin, D.K., Peters, K.E., 1992. Early generation characteristics of a sulfur-rich Monterey kerogen. American Association of Petroleum Geologists Bulletin 76, 1–13.

Baskin, D.K., 1997. Atomic H/C ratio of kerogen as an estimate of thermal maturity and organic matter conversion. American Association of Petroleum Geologists Bulletin 81, 1437–1450.

Behar, F., Pelet, R., Roucache, J., 1984. Geochemistry of asphaltenes. Organic Geochemistry 6, 587–595.

Behar, F., Vandenbroucke, M., Tang, Y., Marquis, F., Espitalié, J., 1997. Thermal cracking of kerogen in open and closed systems: determination of kinetic parameters and stoichiometric coefficients for oil and gas generation. Organic Geochemistry 26, 321–339.

Behar, F., Beaumont, V., Penteado, H.L.B., 2001. Rock-Eval 6 technology: performances and developments. Oil & Gas Science and Technology – Revue de l'Institut Français du Pétrole 56, 111–134.

Behar, F., Lorant, F., Lewan, M., 2008. Role of NSO compounds during primary cracking of a Type II kerogen and a Type III lignite. Organic Geochemistry 39, 1–22.

Behar, F., Roy, S., Jarvie, D., 2010. Artificial maturation of a Type I kerogen in closed system: mass balance and kinetic modelling. Organic Geochemistry 41, 1235–1247.

Bernard, B.B., Brooks, J.M., Sacket, W.M., 1978. Light hydrocarbons in recent Texas continental shelf and slope sediments. Journal of Geophysical Research 83, 4053–4061.

Binotto, R., Rondón, N., Lewan M.D., Santos Neto, E.V., Mendonça Filho, J.G., Spigolon, A.L.D., 2010. Insights on biomarker parameters of the Tremembé Formation (Type I kerogen), Brazil, based on hydrous pyrolysis experiments. Abstracts. 27th Annual Meeting of the Society for Organic Petrology (TSOP), Denver (CO), USA.

Blanc, Ph., Connan, J., 1993. Crude oils in reservoirs: the factors influencing their composition. In: Bordenave, M.L. (Ed.), Applied Petroleum Geochemistry. Editions Technip, Paris, pp. 151–174.

Bordenave, M.L., Espitalié, J., LePlat, P., Oudin, J.L., Vandenbroucke, M., 1993. Screening techniques for source rock evaluation. In: Bordenave, M.L. (Ed.), Applied Petroleum Geochemistry. Editions Technip, Paris, pp. 217–278 (chapter 2).

Cassani, F., Eglinton, G., 1986. Organic geochemistry of Venezuelan extra-heavy oils, 1. Pyrolysis of asphaltenes: a technique for the correlation and maturity evaluation of crude oils. Chemical Geology 56, 167–183.

Chagas, D.B., Assine, M.L., Freiras, F.I., 2007. Fácies sedimentares e ambientes deposicionais da Formação Barbalha no Vale do Cariri, Bacia do Araripe, Nordeste do Brasil. Geociências 26, 313–322.

di Primio, R., Dieckmann, V., Mills, N., 1998. PVT and phase behavior analysis in petroleum exploration. Organic Geochemistry 29, 207–222.

di Primio, R., Horsfield, B., Veja, M.A., 2000. Determining the temperature of petroleum formation from the kinetic properties of petroleum asphaltenes. Nature 406, 173–176.

di Primio, R., Horsfield, B., 2006. From petroleum-type organofacies to hydrocarbon phase prediction. American Association of Petroleum Geologists Bulletin 90, 1031–1058.

Duppenbecker, S., Horsfield, B., 1990. Compositional information for kinetic modelling and petroleum type prediction. Advances in Organic Geochemistry 1989. Organic Geochemistry 16, 259–266.

Engler, K.O.V., 1913. Die Chemic Und Physik Des Erdols, vol. 1. S. Hirzel.

Espitalié, J., Deroo, G., Marquis, F., 1985. La pyrolysis Rock Eval et ses applications. Revue de L'Institut Français du Pétrole 40, 755–784.

Espitalié, J., 1986. Use of T_{max} as a maturation index for different types of organic matter. Comparison with vitrinite reflectance. In: Burrus, J. (Ed.), Thermal Modelling in Sedimentary Basins. Technip, pp. 475–496 (chapter 3, Part A).

Evans, C.R., Rogers, M.A., Bailey, N.J.L., 1971. Evolution and alteration of petroleum in western Canada. Chemical Geology 8, 147–170.

Franks, A.J., Goodier, B.D., 1922. Preliminary study of the organic matter of Colorado oil shales. Quarterly of the Colorado School of Mines 77, 3.

Guthrie, J., Nino, C., and Hassan, H., 2012. Integrating geochemistry, charge rate and timing, trap timing, and reservoir temperature history to model fluid properties in the Frade and Roncador fields, Campos Basin, Offshore Brazil. In: Peters, K.E., Curry, D.J., Kacewicz, M. (Eds.), Basin Modeling: New Horizons in Research and Applications, American Association of Petroleum Geologists Hedberg Series No. 4, 293–315.

Hashimoto, A.T., Appi, C.J., Soldan, A.L., Cerqueira, J.R., 1987. O neo-Alagoas nas Bacias do Ceara, Araripe e Potiguar (Brasil); caracterização estratigráfica e paleoambiental. Revista Brasileira de Geociências 17, 118–122.

Huizinga, B.J., Aizenshtat, Z.A., Peters, K.E., 1988. Programmed pyrolysis–gas chromatography of artificially mature Green River kerogen. Energy and Fuels 2, 74–81.

Horsfield, B., Disko, U., Leistner, F., 1989. The micro-scale simulation of maturation: outline of a new technique and its potential applications. Geologische Rundschau 78, 361–374.

Hunt, J.M., 1996. Petroleum Geochemistry and Geology, second ed. W.H. Freeman and Company, New York.

Jarvie, D.M., 1991. Total organic carbon (TOC) analysis. In: Merrill, R.K. (Ed.), Treatise of Petroleum Geology: Handbook of Petroleum Geology, Source and Migration Processes and Evaluation Techniques. American Association of Petroleum Geologists, pp. 113–118.

Katz, B.J., Mello, M.R., 2000. Petroleum Systems of South Atlantic Marginal Basins – An Overview. In: Mello, M.R., Katz, B.J. (Eds.). Petroleum systems of the South Atlantic Margin. American Association of Petroleum Geologists Memoir 73, 1–13.

Khavari-Khorasani, G., Dolson, J.C., Michelsen, J.K., 1998. The factors controlling the abundance and migration of heavy versus light oils, as constrained by data from the Gulf of Suez. Part I. The effect of expelled petroleum composition, PVT properties and petroleum system geometry. Organic Geochemistry 29, 255–282.

Kotarba, M.J., Curtis, J.B., Lewan, M.D., 2009. Comparison of natural gases accumulated in Oligocene strata with hydrous pyrolysis from Menilite Shales of the Polish Outer Carpathians. Organic Geochemistry 40, 769–783.

Kotarba, M.J., Lewan, M.D., 2013. Sources of natural gases in Middle Cambrian reservoirs in Polish and Lithuanian Baltic Basin as determined by stable isotopes and hydrous pyrolysis of Lower Palaeozoic source rocks. Chemical Geology 345, 62–76.

Lewan, M.D., 1978. Laboratory classification of very fine grained sedimentary rocks. Geology 6 (12), 745–748.

Lewan, M.D., Winters, J.C., McDonald, J.H., 1979. Generation of oil-like pyrolyzates from organic-rich shales. Science 203, 897–899.

Lewan, M.D., 1980. Geochemistry of Vanadium and Nickel in Organic Matter of Sedimentary Rocks (Ph.D. dissertation), University of Cincinnati, 353 pp.

Lewan, M.D., 1983. Effects of thermal maturation on stable organic carbon isotopes as determined by hydrous pyrolysis of Woodford Shale. Geochimica et Cosmochimica Acta 47, 1471–1479.

Lewan, M.D., 1985. Evaluation of petroleum generation by hydrous pyrolysis experimentation. Philosophical Transactions of the Royal Society of London A315, 123–134.

Lewan, M.D., 1987. Petrographic study of primary petroleum migration in the Woodford Shale and related rock units. In: Doligez, B. (Ed.), Migration of Hydrocarbons in Sedimentary Basins. Editions Technip, Paris, pp. 113–130.

Lewan, M.D., 1993a. Laboratory simulation of petroleum formation-hydrous pyrolysis. In: Engel, M., Macko, S. (Eds.), Organic Geochemistry – Principles and Applications. Plenum Press, New York, pp. 419–442.

Lewan, M.D, 1993b. Identifying and understanding suppressed vitrinite reflectance through hydrous pyrolysis experiments. Abstract. Tenth Annual Meeting of the Society for Organic Petrology 10, pp. 1–3.

Lewan, M.D., 1994. Assessing natural oil expulsion from source rocks by laboratory pyrolysis. In: Magoon, L., Dow, W. (Eds.), The Petroleum System Source to Trap, vol. 60. American Association of Petroleum Geologists Memoir, pp. 201–210.

Lewan, M.D., Comer, J.B., Hamilton-Smith, T., Hausenmuller, N.R., Guthrie, J.M., Hatch, J.R., Gautier, D.L., Frankie, W.T., 1995. Feasibility study on material-balance assessment of petroleum from the New Albany Shale in the Illinois Basin, vol. 2137. U.S. Geological Survey Bulletin, 31 pp.

Lewan, M.D., 1997. Experiments on the role of water in petroleum formation. Geochimica et Cosmochimica Acta 61, 3691–3723.

Lewan, M.D., 1998. Sulphur-radical control on petroleum formation rates. Nature 391, 164–166.

Lewan, M.D., Henry, A.A., 2001. Gas:oil ratios for source rocks containing Type-I, -II, -IIs, and -III kerogens as determined by hydrous pyrolysis. In: Dyman, T.S., Kuuskraa, V.A. (Eds.), Geologic Studies of Deep Natural Gas Resources. USGS Digital Data Series DDS-67, version 1.0.

Lewan, M.D., Ruble, T.E., 2002. Comparison of petroleum generation kinetics by isothermal hydrous and non isothermal open-system pyrolysis. Organic Geochemistry 33, 1457–1475.

Lewan, M.D., Kotarba, M.J., Curtis, J.B., Wieclaw, D., Kosakowski, P., 2006. Oil-generation kinetics for organic facies with Type-II and -IIS kerogen in the Menilite Shales of the Polish Carpathians. Geochimica et Cosmochimica Acta 70, 3351–3368.

Lewan, M.D., Roy, S., 2011. Role of water in hydrocarbon generation from Type-I kerogen in Mahogany oil shale of the Green River Formation. Organic Geochemistry 42, 31–41.

Lima, M.R., Perinotto, J.A.J., 1984. Palinologia de sedimentos da parte superior da Formação Missão Velha, Bacia do Araripe. Geociências 3, 67–76.

Lorrant, F., Prinzhofer, A., Behar, F., Huc, A.Y., 1998. Carbon isotopic and molecular constraints on the formation and the expulsion of thermogenic hydrocarbon gases. Chemical Geology 147, 249–264.

Martin, R.L., Winters, J.C., Williams, J.A., 1963. Distribution of n-paraffins in crude oils and their implications to origin of petroleum. Nature 199, 110–113.

Momper, J.A., 1978. Oil migration limitations suggested by geological and geochemical considerations. In: Physical and Chemical Constraints on Petroleum Migration, vol. 1. American Association of Petroleum Geologists Short Course Note Series 8, pp. B1–B60.

Monthioux, M., Landais, P., Monin, J.C., 1985. Comparison between natural and artificial maturation series of humic coals from the Mahakam delta, Indonesia. Organic Geochemistry 8, 275–292.

Mukhopadhyay, P.K., John, A.W., Kruge, M.A., 1995. Organic facies and maturation of Jurassic/Cretaceous rocks, and possible oil-source rock correlation based on pyrolysis of asphaltenes, Scotian Basin, Canada. Organic Geochemistry 22, 85–104.

Muscio, G.P.A., Horsfield, B., 1996. Neoformation of inert carbon during the natural maturation of a marine source rock; Bakken Shale, Williston Basin. Energy Fuel 10, 10–18.

Orr, W.L., 1986. Kerogen/asphaltene/sulfur relationships in sulfur-rich Monterey oils. Organic Geochemistry 10, 499–516.

Orr, W.L., 2001. Evaluating kerogen sulfur content from crude oil properties. In: Isaacs, C.M., Rullkötter, J. (Eds.), The Monterey Formation from Rocks to Molecules. Columbia University Press, New York, pp. 348–367.

Oudin, J.L., 1993. Head-space gas analysis. In: Bordenave, M.L. (Ed.), Applied Petroleum Geochemistry. Editions Technip, Paris, pp. 271–278.

Penteado, H.L.B., Araujo, L.M., 2012. Petroleum systems modeling advances applied in the recent discoveries made in Brazilian marginal basins. AAPG Hedberg Conference Petroleum Systems: Modeling the Past, Planning the Future, Nice, France, October 1–5, 2012.

Prinzhofer, A., Huc, A.Y., 1995. Genetic and post-genetic molecular and isotopic fractionations in natural gases. Chemical Geology. 126, 281–290.

Prinzhofer, A., Mello, M.R., Takaki, T., 2000. Geochemical characterization of natural gas: a physical approach and its applications in maturity and migration estimates. American Association of Petroleum Geologists Bulletin 84, 1152–1172.

Quigley, T.M., Mackenzie, A.S., 1988. The temperatures of oil and gas formation in the subsurface. Nature 33, 549–552.

Radke, M., Horsfield, B., Littke, R., Rullkötter, J., 1997. Maturation and petroleum generation. In: Welte, D.H., Horsfield, B., Baker, D.R. (Eds.), Petroleum and Basin Evolution. Springer-Verlag, Berlin-Heidelberg, pp. 171–229.

Ruble, T.E., 1996. Geochemical Investigation of the Mechanism of Hydrocarbon Generation and Accumulation in the Uinta Basin, Utah (Ph.D. dissertation), University of Oklahoma, Norman, OK.

Ruble, T.E., Lewan, M.D., Philp, R.P., 2001. New insights on the Green River petroleum system in the Uinta basin from hydrous pyrolysis experiments. American Association of Petroleum Geologists Bulletin 85, 1333–1371.

Rudkiewicz, J.L., Behar, F., 1994. Influence of kerogen type and TOC content on multiphase primary migration. Organic Geochemistry 21, 121–133.

Sagjo, C.S., 1980. Hydrocarbon generation super-thick Neogene sequence in south-east Hungary. A study of the extractable organic matter. In: Douglas, A.G., Maxwell, J.R. (Eds.), Advances in Organic Geochemistry 1979. Pergamon Press, London, pp. 103–113.

Sandvik, E.I., Young, W.A., Curry, D.J., 1992. Expulsion from hydrocarbon sources: the role of organic absorption. Organic Geochemistry 19, 77–87.

Santamaría-Orozco, D., Horsfield, B., 2003. Gas generation potential of upper Jurassic (Tithonian) source rocks in the Sonda de Campeche, Mexico. In: Bartolini, C., Buffler, R.T., Blickwede, J. (Eds.), The Circum-Gulf of Mexico and the Caribbean: Hydrocarbon Habitats, Basin Formation, and Plate Tectonics, vol. 79. American Association of Petroleum Geologists Memoir, USA, pp. 349–363.

Schimmelmann, A., Lewan, M.D., Winsch, R.P., 1999. D/H isotope ratios of kerogen, bitumen, oil, and water in hydrous pyrolysis of source rocks containing kerogen types I, II, IIS, and III. Geochimica et Cosmochimica Acta 63, 3751–3766.

Schimmelmann, A., Boudou, J.P., Lewan, M.D., Wintsch, R.P., 2001. Experimental controls on D/H and $^{13}C/^{12}C$ ratios of kerogen, bitumen and oil during hydrous pyrolysis. Organic Geochemistry 32, 1009–1018.

Schoell, M., 1983. Genetic characterization of natural gases. American Association of Petroleum Geologists Bulletin 67, 2225–2238.

Seewald, J.S., Benitez-Nelson, B.C., Whelan, J.K., 1998. Laboratory and theoretical constraints on the generation and composition of natural gas. Geochimica et Cosmochimica Acta 62, 1599–1617.

Soldan, A.L., Santos Neto, E.V., Cerqueira, J.R., Concha, F.J.M., Branco, V.A.C., Arai, M., 1988. Hydrous-pyrolysis: a tool to access maturation. Boletim de Geociências da Petrobras 2, 65–76.

Souza, I.V.A.F., Araújo, C.V., Menezes, T.R., Coutinho, L.F.C., Binotto, R., Spigolon, A.L.D., Fontes, R.A., Santos Neto, E.V., Rondon, N.D.V.F., Mendonça Filho, J.G., 2014. Organic and mineral matter changes due to oil generation, saturation and expulsion process based on artificial maturation experiments. Geologica Acta 12, 351–362.

Spigolon, A.L.D., Cerqueira, J.R., Binotto, R., Fontes, R.A., Silva, T.F., Bautista, D.F.G., 2010. Source rock characteristics predicted based on MSSV pyrolysis of asphaltenes from a severely biodegraded oil. Revista Latino Americana de Geoquímica Orgânica 1, 14–24.

Spigolon, A.L.D., Lewan, M.D., Mendonça Filho, J.G., Penteado, L.H.B., Coutinho, F.C., 2013. New insights on changes in the oil quality during petroleum formation by hydrous pyrolysis on a Brazilian source rock containing Type-I kerogen. In: Abstracts. 26th International Meeting on Organic Geochemistry 1, Costa Adeje, Tenerife, Spain, pp. 417–418.

Tan, J., Horsfield, B., Mahlstedt, N., Zhang, J., di Primio, R., Tiem Vu, T.A., Boreham, C.J., van Graas, G., Tocher, B.A., 2013. Physical properties of petroleum formed during maturation of Lower Cambrian shale in the upper Yangtze Platform, South China, as inferred from phase kinetics modeling. Marine and Petroleum Geology 48, 47–56.

Tissot, B.P., 1969. Premières données sur les mécanismes et la cinétique de la formation du pétrole dans les sédiments. Simulation d'un schéma réactionnel sur ordinateur. Revue de l'Institut Francais du Petrole 24, 470–501.

Tissot, B., Califet-Debyser, Y., Deroo, G., Oudin, J.L., 1971. Origin and Evolution of Hydrocarbons in Early Toarcian Shales, Paris Basin, France. American Association of Petroleum Geologists Bulletin 55, 2177–2193.

Tissot, B.P., Espitalié, J., 1975. L'évolution thermique de la matière organique des sédiments: application d'une simulation mathématique. Revue de l'Institut Francais du Petrole 30, 743–777.

Tissot, B.P., Welte, D.H., 1984. Petroleum Formation and Occurrence, second ed. Springer-Verlag, Berlin.

Tissot, B.P., Pelet, R., Ungerer, P., 1987. Thermal history of sedimentary basins, maturation indices and kinetics of oil and gas formation. American Association of Petroleum Geologists Bulletin 71, 1445–1466.

Tyson, R.V., 1995. Sedimentary Organic Matter. Chapman & Hall, London.

Utah Geologic Survey, 2014, Cumulative oil production reported for Duchesne and Uintah counties, Utah. <http://oilgas.ogm.utah.gov/pub/Publications/Reports/Prod/County/Cty_Oct_2014.pdf>.

Winters, J.C., Williams, J.A., Lewan, M.D., 1983. A laboratory study of petroleum generation by hydrous pyrolysis. In: Bjorøy, M. (Ed.), Advances in Organic Geochemistry 1981. John Wiley & Sons, New York, pp. 24–533.